

1 This is the pre-peer reviewed version of the following article: [J. Reolid; C. Betzler. The  
2 ichtnology of carbonate drifts. *Sedimentology*. 66, pp. 1427 - 1448. 2019.], which has been  
3 published in final form at [<http://doi.org/10.1111/sed.12563>]. This article may be used for non-  
4 commercial purposes in accordance with Wiley Elsevier Terms and Conditions for Use of Self-  
5 Archived Versions

6

## 7 **Abstract**

8 Carbonate drifts have so far not been as intensely investigated as their siliciclastic equivalents,  
9 especially from an ichtnological perspective. The aim of this work is therefore to provide an  
10 overview of the different bioturbation styles in carbonate drifts for ichtnologists and  
11 sedimentologists working in such deposits. Different types of carbonate drifts from the  
12 Maldives were studied to address this objective. The cores recovered during IODP Expedition  
13 359 were examined to provide the sedimentological and ichtnological data for a detailed analysis  
14 of the ichtnology of carbonate drifts. The ichtnological characteristics of the Maldives drifts are  
15 compared to other carbonate drifts in order to discuss similarities and differences and thus  
16 provide an overview of the general characteristics of carbonate drift ichtnology. These drifts are  
17 located in the Santaren Channel which lines Great Bahama Bank, along the Marion Plateau in  
18 Australia, in the Limassol and Larnaca basins in Cyprus, and in the Danish Basin in Denmark.  
19 The common characteristics of bioturbation in carbonate drifts are (1) the complete bioturbation  
20 of the sediment with bioturbation indexes between 4 and 6, (2) the occurrence of distinctive  
21 trace fossils limited to facies contacts or condensed intervals, (3) a typical ichnoassemblage  
22 consisting of *Thalassinoides*, *Scolicia*, *Planolites*, *Zoophycos*, *Chondrites*, *Phycosiphon*, and  
23 *Palaeophycus*, (4) the contiguous occurrence of ichnogenera from different tiers, with only  
24 *Zoophycos* and *Chondrites* as deep tiers, (5) distinct infills of the traces including particulate  
25 organic-matter, pyrite, silica, and celestine. In addition, the main ichnofacies of carbonate drifts

26 is the *Zoophycos* ichnofacies. Ichnofabrics grade from coarse-grained and completely  
27 bioturbated to ichnofabrics with present to rare trace fossils and preserved sedimentary  
28 structures. The type and intensity of the bioturbation is controlled by the amount of organic  
29 matter and the oxygenation at the seafloor that is determined by the action of bottom currents  
30 and the sea-level fluctuations affecting the carbonate factory in carbonate platforms bordering  
31 the basins where the carbonate drifts form. The study of the bioturbation in core and outcrop  
32 provides paleoenvironmental information about carbonate-drift deposits that complement the  
33 classical sedimentological data.

34 **Keywords:** Ichnofacies, Ichnofabrics, Bioturbation, Contourites, Periplatform carbonates

## 35 1. INTRODUCTION

36 Drifts are important sedimentary environments because they record paleoclimatological and  
37 paleoceanographical information at a higher resolution than does pelagic background  
38 sedimentation (Rebesco, 2005; Rebesco *et al.*, 2014). Carbonate drifts have up to now not been  
39 as broadly investigated as their siliciclastic equivalents (Stow *et al.*, 2002; Viana and Rebesco,  
40 2007; Rebesco and Camerlenghi, 2008; Rebesco *et al.*, 2014). Several studies, however,  
41 document their importance in the development of tropical carbonate platform edifices (Mullins  
42 *et al.*, 1980; Anselmetti *et al.*, 2000; Isern *et al.*, 2004; Betzler *et al.*, 2009, 2013, 2014; Eberli  
43 *et al.*, 2010; Lüdmann *et al.*, 2012, 2013; Mulder *et al.*, this volume; Paulat *et al.*, this volume).  
44 Studies on the ichnology of siliciclastic drifts have demonstrated that such deposits are  
45 characterized by a high degree of bioturbation (Stow *et al.*, 1998, 2002; Wetzel *et al.*, 2008;  
46 Rebesco *et al.*, 2014; Rodríguez-Tovar and Hernández-Molina, 2018). The study of the  
47 bioturbation in drifts may be of interest to paleoenvironmental, paleoceanographical, and  
48 paleoclimatological interpretation of the drift deposits as well as for their characterization as  
49 hydrocarbon reservoirs (Rodríguez-Tovar and Hernández-Molina, 2018).

50 Understanding of bioturbation in carbonate drifts is very limited and is mostly focused on the  
51 problems of such deposits in relative to their siliciclastic counterparts, especially in terms of  
52 masking of the primary structures by diagenesis (Kahler and Stow, 1998; Hüneke and Stow,  
53 2008). The aim of this work is therefore to provide an overview of the different bioturbation  
54 styles in carbonate drifts and to establish a background for ichnologists and sedimentologists  
55 working in such deposits.

56 For addressing these objectives, different types of carbonate drifts from the Maldives were  
57 studied, as the Maldives can be considered as a type locality for carbonate drifts (Lüdmann *et*  
58 *al.*, 2013, 2018). There, in the deep-water realm of the Inner Sea giant elongated drift bodies  
59 have formed since the Miocene. They exhibit geometries and seismic characteristics  
60 comparable to their siliciclastic counterparts, including mounded shapes and associated moats  
61 (Lüdmann *et al.*, 2013). Cores from these carbonate drifts were recovered during the cruise  
62 M74/4 NEOMA (Betzler *et al.*, 2013) and during the International Ocean Discovery Program  
63 (IODP) Expedition 359 (Betzler *et al.*, 2016, 2017, 2018). These cores provide  
64 sedimentological and ichnological data for a detailed analysis of the ichnology of carbonate  
65 drifts. The ichnological characteristics of the Maldives drifts are compared with other carbonate  
66 drifts from the Santaren Channel lining Great Bahama Bank, the Marion Plateau in eastern  
67 Australia, the Limassol and Larnaca basins in Cyprus, and the Danish Basin in Denmark (Fig.  
68 1A) to assess similarities and differences and thus provide an overview of general  
69 characteristics of carbonate drift ichnology. We present a compilation of different bioturbation  
70 styles in carbonate drifts and provide the base for further detailed studies on their  
71 paleoenvironmental conditions.

## 72 **2. GEOLOGICAL SETTING**

73 The Maldives archipelago in the central equatorial Indian Ocean is a 3-km-thick isolated  
74 tropical-carbonate edifice located southwest of India (Fig. 1B; Aubert and Droxler, 1992; Purdy

75 and Bertram, 1993). The carbonates formed on an early Paleogene (60–50 Ma) faulted volcanic  
76 basement (Duncan and Hargraves, 1990). Carbonate drifts in the Maldives archipelago have  
77 been developed since ~ 13 Ma (Betzler *et al.*, 2009, 2016, 2018; Lüdmann *et al.*, 2013) and are  
78 arranged in 10 depositional sequences (ds1-ds10) defined by their respective lower boundaries  
79 DS1-DS10 (Lüdmann *et al.*, 2013; Betzler *et al.*, 2016, 2017, 2018). In the Maldives, there are  
80 three main types of carbonate drifts according to their geometries, internal structure, and  
81 composition including mounded drifts (Fig. 2B) and delta drifts (Fig. 2C) close to the drowned  
82 platforms, as well as sheeted drifts and dunes in the Inner Sea and channels among atolls  
83 (Betzler *et al.*, 2018, Fig. 2C). Delta drift deposits comprise ds1 to ds4 in the proximal areas of  
84 the Inner Sea (Fig. 2C). These drift bodies deposited at the exit of passages through the drowned  
85 parts of the platform, while remaining banks and atolls continued to grow (Betzler *et al.*, 2009,  
86 2013; Lüdmann *et al.*, 2013). Lobes were fed by easterly currents and reworked by a current  
87 system flowing obliquely or normally to this main stream and the sediment accumulated by this  
88 current system progressively filled the Inner Sea from west to east (Lüdmann *et al.*, 2013). In  
89 the distal areas of the Inner Sea and in the proximal areas from ds3 to ds10, sheeted drifts and  
90 submarine dunes occur (Betzler *et al.*, 2013; Lüdmann *et al.*, 2013). Starting with seismic  
91 sequence ds6, at the end of the Messinian, the opening of a southern gateway introduced  
92 northward flow of bottom currents into the Inner Sea, resulting in the deposition of giant  
93 elongated drifts attached to the eastern flank of the basin, filling it from east to west (Lüdmann  
94 *et al.*, 2013). Detached drifts form at the downcurrent flanks of the atolls (Betzler *et al.*, 2009,  
95 2013), and the currents controlling the drift deposition in the Maldives prevail during the  
96 Quaternary (Betzler *et al.*, 2013; Reolid *et al.*, 2017; Bunzel *et al.*, 2017). The water depth at  
97 what the drifts were deposited changed through time from ~50 m at the time of the delta drift  
98 deposition (Reolid *et al.*, this volume) to ~500 m in present day (Betzler *et al.*, 2017).

99 The Bahamas archipelago is a carbonate province consisting of several isolated platforms  
100 situated on the southern end of the eastern continental margin of the United States. In the  
101 Santaren Channel, at a water depth of ~600-700 m and ~30 km from the western platform edge  
102 of the Great Bahama Bank, there is a continuous drift sequence of Neogene to present-day in  
103 age that interfingers with prograding carbonate-bank deposits of the Bahamas (Eberli *et al.*,  
104 1997; Kroon *et al.*, 2000; Anselmetti *et al.*, 2000; Bergman *et al.*, 2010; Paulat *et al.*, this  
105 volume).

106 The Marion Platform in northeastern Australia was a large carbonate edifice that drowned  
107 during the Middle-Late Miocene (John and Mutti, 2005; Eberli *et al.*, 2010). A system of  
108 carbonate drifts has since then dominated the sedimentation on the Marion Plateau (John and  
109 Mutti, 2005; Eberli *et al.*, 2010). These drift deposits are Late Miocene to present-day in age  
110 and were deposited at water depths of more than 200 m (Eberli *et al.*, 2010).

111 In the area of Cyprus, deep-sea sediments started to deposit over the Cretaceous oceanic crust  
112 between the Maastrichtian and early Miocene, first as turbidites and later on as slow pelagic  
113 deposition (Stow *et al.*, 2002; Hüneke and Stow, 2008). During the latest Eocene to early  
114 Miocene the deposition was affected by the influence of bottom currents (Kahler and Stow,  
115 1998). The water depth at the time of the drift deposition was in the range of 2000-3000 m  
116 (Stow *et al.*, 2002).

117 The Maastrichtian chalk in Denmark spreads over a large extension of Denmark and the North  
118 and Baltic sea. It is of pelagic origin and was permanently affected by the action of bottom  
119 currents that resulted in mounded drifts, a sediment wave complex, and an elongate moat-drift  
120 system (Anderskov *et al.*, 2007; Surlyk and Lykke-Andersen, 2007; Damholt and Surlyk,  
121 2004). The water depth of the sea was of several hundred meters with up to 800 m in the deepest  
122 areas of the Danish Basin, well below the photic zone (Lauridsen *et al.*, 2011).

### 123 3. MATERIALS AND METHODS

124 During the IODP Expedition 359 Sites U1466, U1467, U1468, and U1471 were cored in the  
125 Inner Sea to recover a sedimentary sequence encompassing a carbonate drift succession  
126 (Miocene to Pleistocene). Core retrieval, handling and all on board measurements including  
127 downhole logging and core to seismic correlation are described in detail in Betzler *et al.* (2017).  
128 The characterization of the different slope, drift, and basinal facies as well as the first approach  
129 to the bioturbation at the study sites relies on preliminary on-board visual core descriptions and  
130 later detailed analysis of high-resolution photographs obtained by the Section Half Imaging  
131 Logger (SHIL), which captures continuous high-resolution images (Betzler *et al.*, 2017). These  
132 data were backed up with the petrographic analysis of circa 200 thin-sections to identify  
133 microfacies and components. The nomenclature for the facies and microfacies of carbonate  
134 rocks follows Dunham (1962) and Embry and Klovan (1974). The age assignments of the  
135 succession rely on calcareous nannoplankton and planktonic foraminifer events (Betzler *et al.*,  
136 2016, 2017). The natural gamma radiation from downhole logs (HSGR) and core measurements  
137 (NGR) was used to characterize the organic-matter content of the sediment according to Betzler  
138 *et al.* (2016) and Reolid and Betzler (2018). The piston core NEOMA 1143 was retrieved during  
139 RV Meteor cruise M74/4 and has a length of 12.95 m (Betzler *et al.*, 2013). It was divided into  
140 two halves, photographed, and studied for sedimentology and ichnology.

141 The ichnological study of the carbonate drifts of the Maldives was backed up with the data of  
142 carbonate drifts from Bahamas, the Marion Plateau, Cyprus, and the Danish Basin (Fig. 1A).  
143 In Bahamas, at ODP Site 1006A (20°23.989'N, 79°27.541'W), the studied interval is Miocene  
144 to Pliocene in age and comprised cores 37X to 75X, 330.6 to 698.1 mbsf. The studied drift  
145 intervals from the Marion Plateau at ODP Sites 1192A (20°34.306'S, 152°24.257'E) and 1195B  
146 (20°24.283'S, 152°40.243'E) span from cores 5H to 15H (29.5 to 125.5 mbsf) and cores 5H to  
147 13H (36.9 to 122.4 mbsf) respectively. These drifts are Late Miocene to Pliocene in age. The

148 drift deposits of Cyprus were studied at the Miocene Lymbia (34°59.5'N, 33°28.7'E) and Petra  
149 Tou (34°39.7'N, 32°39.1'E) sections. A nice example of the Maastrichtian chalk deposits in the  
150 Danish Basin crops out in Stevns Klint (55°18'N, 12°26.8'E).

151 The systematic ichnological analysis was conducted on digitally-enhanced (light, contrast, and  
152 color) high-resolution images of core section halves (Reolid and Betzler, 2018). The analysis  
153 was continuous, section-by-section, for the IODP and ODP sites and spotted in the field  
154 locations of Cyprus (Lymbia and Petra Tou sections) and Denmark (Stevns Klint section).  
155 Unfortunately, for old ODP expeditions there are no high-resolution photographs available in  
156 the data repository, and the ichnological analysis relies on onboard low-resolution core-  
157 photographs, close-ups, and core-descriptions by the onboard sedimentologists. The spotted  
158 field-observations in Cyprus and Denmark were implemented through the available literature  
159 on these drifts. The quantification of the bioturbation intensity follows the method of Taylor  
160 and Goldring (1993). Identification of the main ichnotaxa, measurement of the burrow sizes, of  
161 the tiering, and cross-cutting relationships were also recorded where possible, but  
162 unfortunately, they are not statistically representative. The ichnofabrics were defined according  
163 to the bioturbation index, the ichnoassemblage, and the sediment type (Reolid and Betzler,  
164 2018).

## 165 **4. RESULTS**

### 166 **4.1 Maldives carbonate drifts**

167 The texture, composition, and ichnology of the drift successions at Sites U1466, U1467, U1468,  
168 and U1471 change from proximal to distal settings, and from the northern to the southern part  
169 of the Kardiva Channel (Fig. 1B). A summary of the main drift types and their bioturbation can  
170 be found in Table 1. At Site U1466 and U1468 there are deposits associated with a delta drift  
171 complex that progrades towards the E, i.e. the Inner Sea (ds1 to ds3, Fig. 2; Lüdmann *et al.*,

172 2018). Site U1467 records a succession of sheeted drifts and submarine dunes (ds4 to ds10, Fig.  
173 2). Site U1471 in the southern branch of the Kardiva Channel has deposits associated to the  
174 delta drift and the overlying sheeted drifts. Core NEOMA 1143 retrieved sediment from a  
175 mounded drift (Fig. 2C).

176 The drift deposits of the Maldives overlie the slope and basinal sediments of a partially drowned  
177 Miocene Carbonate platform. The slope to basinal deposits of this platform consist of bioclastic  
178 packstone to wackestone with benthic and planktonic foraminifera. The youngest slope  
179 sediments are intensely bioturbated with indices of 4 to 5 (Fig. 3). Scarce individual burrows  
180 of *Thalassinoides* can be identified out of the mottled background (Reolid and Betzler, 2018).  
181 At Site U1466, the change from the slope to the drift deposits coincides with an abrupt increase  
182 of the degree of bioturbation whereas it is more gradual at Site U1468, i.e. in a more distal slope  
183 position (Fig. 3).

#### 184 4.1.1 IODP Site U1466

185 In the northern branch of the Kardiva Channel, at Site U1466 the delta drift facies consists of  
186 fine-grained packstone to wackestone, locally grainstone, with abundant bioclasts and minor  
187 benthic and planktonic foraminifera. From DS1 up to 200 mbsf the sediment of the delta drift  
188 is completely bioturbated without individual burrows or a mottling texture (Fig. 3A). From 200  
189 to 160 mbsf there is a partially lithified packstone where bioturbation may be expressed as small  
190 lithified-nodules floating in the sediment (Fig. 4B). Towards the top of the delta drift succession  
191 large benthic foraminifera including *Lepidocyclina*, *Miogypsina*, *Operculina*, and *Nummulites*,  
192 together with equinoid remains may be present. In this interval, bioturbation cannot be  
193 determined because of the coarse grain size of the deposits. In the overlying sheeted drift and  
194 sand dunes there are some changes in color and texture that may be interpreted as a bioturbation  
195 (Fig. 4). The bioturbation degree is 5 to 6 and the only traces are likely *Thalassinoides* and are  
196 represented by a bioclastic grainstone with a packstone infill. From 75 mbsf to the sea floor

197 there are local changes in the sediment packing that may be interpreted as biodeformational  
198 features.

#### 199 4.1.2 IODP Site U1468

200 Basinwards, at Site U1468, the delta drift sediments consist of packstone and wackestone that  
201 gradually change upwards into grainstone to rudstone (Fig. 2). Components are abundant silt  
202 sized bioclasts in the lower part and a mixture of large benthic foraminifera and bioclasts  
203 towards the top (Fig. 4). From the base of the drift up to 400 mbsf the sediment is intensely  
204 bioturbated (BI=5-6) with scarcely identifiable burrows of *Thalassinoides* and *Palaeophycus*  
205 (Fig. 3 and 4A.). Above, the bioturbation is so intense that no individual burrows or mottling  
206 texture are observed. This part of the succession contains scattered chert nodules with rounded  
207 to elongated morphologies that could be related to large trace fossils such as *Thalassinoides*  
208 (Fig. 5A). From 300 to 225 mbsf there is a partially lithified wackestone where bioturbation  
209 may be present, represented by small lithified nodules floating in the sediment (Fig. 4B).  
210 Chertified burrows may also occur (Fig. 5A). Between 200 mbsf and 160 mbsf there is a cryptic  
211 mottling texture, and from 160 to 90 mbsf there is an alternation of packstone and grainstone  
212 with abundant large benthic foraminifera where rarely poorly-preserved traces can be observed  
213 (Fig. 4C, F). These traces may correspond to *Thalassinoides* and usually contain abundant  
214 organic matter in their infills (Fig. 5B). This interval is partly mottled. From 90 to 50 mbsf the  
215 grain size is coarse and no bioturbation can be determined.

216 Overlying the delta drift deposits, the sheeted drift at Site U1468 consists of unlithified to  
217 partially lithified planktonic foraminifera-rich packstone to grainstone completely  
218 homogenized by the bioturbation (BI=6; Fig. 4D). Components include mix shallow-water and  
219 pelagic bioclasts including *Halimeda*, echinoids, iron stained intraclasts, otoliths, and pteropods  
220 (Fig. 4G).

### 221 4.1.3 IODP Site U1471

222 In the southern part of the Kardiva Channel, at Site U1471, the deposits of the delta drift are  
223 fine-grained planktonic foraminifera-rich packstone alternating with coarse-grained bioclastic-  
224 rich grainstone. Benthic foraminifera and equinoid remains are common. Large benthic  
225 foraminifera are locally abundant, especially between 890 and 880 mbsf. Packstone intervals  
226 are darker in color, and their thickness ranges between 2 and 35 cm. These intervals have higher  
227 organic content and exhibit wavy and/or finely laminated layering (Fig. 6A). The bioturbation  
228 is intense with indexes around 4-5 in the packstone and 6 in the grainstone intervals (Fig. 6A).  
229 The ichnoassemblage varies upcore starting with *Thalassinoides*, *Planolites*, *Phycosiphon*,  
230 *Zoophycos*, *Chondrites* and minor *Palaeophycus*, with some interval especially rich in  
231 *Phycosiphon*. At 830 mbsf, *Palaeophycus* starts to be more significant, and *Zoophycos*,  
232 *Phycosiphon* and *Chondrites* become accessories.

233 The grainstone layers are lighter in color and are completely homogenized by the intense  
234 bioturbation. Just locally some large *Thalassinoides* can be identified with a packstone infill.  
235 The contacts between the packstone and the grainstone may be sharp, gradual, and eventually  
236 bioturbated, with trace fossils commonly infilled by the coarser material (Fig. 6A). From 805  
237 mbsf up to approximately 615 mbsf the facies consists of an alternation of wackestone and  
238 packstone. The ichnoassemblage is similar to that of the directly underlying interval but the  
239 bioturbation degree is progressively higher upcore (Fig. 6B). In the wackestone intervals it is  
240 possible to identify individual traces in contrast with the completely bioturbated packstone  
241 intervals. In the transition interval from delta to sheeted drift, from 700 to 615 mbsf, the  
242 bioturbation of the sediment is pervasive and just some *Zoophycos* and minor *Palaeophycus*  
243 can be identified out of the mottled background (Fig. 6B). In some intervals, discrete burrows  
244 present infills rich in organic matter (Fig. 5C). From 615 mbsf to the top of the hole, the sheeted  
245 drift facies is mostly a packstone with intercalations of wackestone, both completely

246 homogenized by the bioturbation (Fig. 6C). *Thalassinoides* may be locally identified out of the  
247 background bioturbation and may present celestine infill (Fig. 5D). The uppermost unlithified  
248 sediment commonly displays mottled texture (Fig. 6D).

#### 249 4.1.4 IODP Site U1467

250 At Site U1467 the sheeted drift sediment is a wackestone to packstone with abundant planktonic  
251 foraminifera, silt-sized bioclasts, common benthic foraminifers (locally some *Amphistegina*),  
252 and few to present echinoid spines and particulate organic matter (Fig. 2). Bioturbation is  
253 intense from the base of the hole up to 500 mbsf with common to abundant *Thalassinoides*,  
254 *Scolicia*, *Planolites*, *Zoophycos*, *Chondrites*, and *Palaeophycus* (Fig. 7A). In this part of the  
255 succession, there is an alternation of light and dark sediments. Darker intervals range in  
256 thickness from 1 to 30 cm and represent up to a 30% of the cores. The sediment composition is  
257 similar in both intervals with more bioclasts in the light ones (Fig. 7E) and more organic matter  
258 in the dark intervals (Fig. 7F). The NGR values are higher in the dark intervals but the  
259 bioturbation degree and assemblage are almost identical in the light and dark intervals (Fig. 2).  
260 From 540 to 370 mbsf the contrasts in color are progressively fading. The degree of lithification  
261 of the sediment decreases upcore from lithified to partially lithified (Betzler *et al.*, 2017). The  
262 bioturbation is intense and consists of the same ichnoassemblage as in the underlying interval  
263 with *Zoophycos* being locally dominant (Fig. 7B). In parts, the bioturbation is so intense that it  
264 is not possible to identify individual burrows, locally even the mottling disappears and the  
265 sediment is completely homogenized. From 370 to 200 mbsf burrows are progressively less  
266 significant and biodeformational structures dominate. *Thalassinoides*, *Chondrites*, *Planolites*,  
267 and *Zoophycos* are just locally identifiable in the darker intervals (Fig. 7C). From 200 mbsf to  
268 the sea floor, the bioturbation degree is intense and sediments are mottled or even completely  
269 homogenized, and trace fossils represented by *Thalassinoides* occur in some scattered dark  
270 sediment intervals (Fig. 7D). The sediment in the uppermost part of the hole consists of

271 planktonic foraminifera rich wackestone with some fish debris and scattered large benthos such  
272 as brachiopods and cold-water corals (Fig. 7G).

#### 273 *4.1.5 Core NEOMA 1143*

274 The sediment of the mounded detached drift east of Goidhoo Atoll (Fig. 1B) is mainly a  
275 periplatform ooze with planktonic foraminifera, pteropods, otoliths, mollusk remains, benthic  
276 foraminifera, sponge spicules, echinoid debris, and rare solitary corals (Betzler *et al.*, 2013).  
277 The succession is arranged in alternating light and dark colored greenish to olive gray intervals.  
278 The bioturbation is intense and mostly consists of biodeformational structures. Just locally  
279 individual trace fossils of *Thalassinoides* and ?*Planolites* may be identified out of the mottled  
280 background (Fig. 8).

## 281 **4.2 Other carbonate drifts**

### 282 *4.2.1 Bahamas*

283 The drift sediment consists of fine-grained wackestone to packstone, locally mudstone, with  
284 abundant planktonic foraminifera, benthic foraminifera, bioclasts, peloids, echinoid debris, and  
285 fish remains. There are 110- to 300-cm-thick intervals of alternating darker and lighter sediment  
286 with fish debris better preserved in the dark intervals (Eberli *et al.*, 1997). Firmgrounds are  
287 locally present and may be bioturbated (Fig. 9A). Bioturbation is pervasive throughout the drift  
288 facies homogenizing completely the sediment (Fig. 9B and C). Just in some intervals, and at  
289 the position of the firmgrounds, the bioturbation degree is lower and allows identification of  
290 distinctive burrows out of the mottled background including *Thalassinoides*, *Chondrites*, and  
291 *Planolites*. Larger burrows are up to 1-2 cm in diameter. Grains inside the burrows may be  
292 pyritized, especially the planktonic foraminifera (Fig. 9C).

### 293 *4.2.2 Marion Plateau*

294 The recovered drift facies consists of planktonic foraminifera-rich wackestone to mudstone at  
295 the bottom of the drift deposits that change into packstone and grainstone at the top. The  
296 sediment is completely homogenized by the bioturbation and no sedimentary structures are  
297 preserved. The homogenization is especially intense in the coarser grainstone intervals. In the  
298 wackestone and packstone there are alternations of lighter and darker intervals, in response to  
299 variations of the clay content that locally allow the recognition of individual trace fossils out of  
300 the mottled background. The burrows may be stained black from finely disseminated pyrite  
301 and/or particulate organic matter (Fig. 9D). There are firmgrounds where the trace fossils  
302 present distinct sediment infill (Fig. 9E). Among the identifiable trace fossils there are  
303 *Thalassinoides*, *Zoophycos* (Fig. 9F), and rarely *Scolicia* and *Chondrites*.

#### 304 4.2.3 Cyprus

305 Stow *et al.* (2002) described part of the late Oligocene early Miocene Lefkara Formation in  
306 Cyprus as a type example of a carbonate contourite deposit. The calcilutite/calcsiltite to marly  
307 calcilutite of the Lymbia and Petra Tou sections are well bedded with up to 30-cm thick beds  
308 that can be massive, finely-parallel laminated, or with lenticular bedding (Hüneke and Stow,  
309 2008). The sediment consists of fine-grained planktonic-foraminifera wackestone to packstone  
310 with rare equinoid fragments and fish remains. The facies is locally mudstone, which is  
311 interpreted to reflect minor current winnowing (Stow *et al.*, 2002). The sediment is completely  
312 bioturbated except for intervals with a fine parallel lamination. Individual traces are medium to  
313 poorly preserved. Where visible, the main ichnoassemblage consists of *Thalassinoides*,  
314 *Chondrites*, *Planolites*, and *Zoophycos* with *Ophiomorpha* and ?*Helminthoides* also present  
315 (Hüneke and Stow, 2008; Rodríguez-Tovar and Hernández-Molina, 2018). The diagenesis of  
316 the carbonates may have obscured the recognition of the facies and trace fossils (Hüneke and  
317 Stow, 2008).

#### 318 4.2.4 Denmark

319 The drift deposits consist of fine-grained chalk made out of the debris of coccolithophorid algae  
320 as well as planktonic foraminifera, calcispheres and skeletal remains of minute suspension-  
321 feeding invertebrates (Surlyk and Lykke-Andersen, 2007). The facies displays a cyclicity  
322 consisting of decimeter-thick bioturbated beds alternating with slightly thinner non-bioturbated,  
323 mainly laminated beds (Damholt and Surlyk, 2004). The bioturbated beds contain diverse trace  
324 fossils including common *Zoophycos*, *Chondrites*, *Planolites*, *Thalassinoides* and *Phycosiphon*.  
325 *Asterosoma* may be present but its identification is equivocal. *Thalassinoides* may be locally  
326 abundant and preserved in chert concretions (Anderskov *et al.*, 2007). The laminated beds lack  
327 syndepositional bioturbation and only contain scattered well-preserved deep-tier *Zoophycos*  
328 and locally also thin *Chondrites* penetrating downwards from the overlying bioturbated units  
329 (Damholt and Surlyk, 2004).

## 330 **5. DISCUSSION**

### 331 **5.1 Main ichnological features in carbonate drifts**

332 A list of the main ichnological features in carbonate drifts is presented in Table 2. The first  
333 feature that all carbonate drifts do have in common is the intense and pervasive bioturbation.  
334 This is also a diagnostic element of siliciclastic and mixed carbonate-siliciclastic drifts (Stow,  
335 2002; Stow and Faugères, 2008; Rebesco *et al.*, 2014; Alonso *et al.*, 2016; Dorador and  
336 Rodríguez-Tovar, 2016). The intense bioturbation ranges from mottling that destroys pre-  
337 existing sedimentary structures to complete homogenization of the sediment (Pemberton *et al.*,  
338 2008). The intensity of a bioturbation is a criterion that allows the differentiation of carbonate  
339 drift deposits from other periplatform deposits (Fig. 3). The intensity of bioturbation of  
340 carbonate drifts is apparently dependent of the sediment grain size. Coarse-grained sediment,  
341 grainstone and rudstone, displays a bioturbation degree slightly higher than intervals of silt-  
342 sized wackestone and mudstone (Figs. 4 and 6). But in any case, the bioturbation degree in the  
343 fine-grained facies is also high. Similar intensity of bioturbation in fine-grained drifts is also

344 reported from chalk deposits of the Danish drifts (Anderskov *et al.*, 2007; Rasmussen and  
345 Surlyk, 2012).

346 Not only the intense bioturbation, but also the homogeneity of some facies, with respect to the  
347 mineralogy and grain composition, results in little to no sediment-color contrast between the  
348 burrow infill and the background sediment (Knaust *et al.*, 2012). This additionally hinders the  
349 recognition of individual trace fossils in carbonate drifts, and the contrast may even be obscured  
350 by diagenesis (Hüneke and Stow, 2008).

351 Two general types of bioturbation can be distinguished in carbonate drifts: (1) Trace fossils  
352 with sharp outlines and characteristic recurrent geometries that allow their classification in  
353 terms of ichnotaxonomy, and (2) biodeformational structures with more diffuse outlines and  
354 non-recurrent geometry. The occurrence of discrete trace fossils is mostly restricted to some  
355 horizons, such as the transitions between lighter and darker colored intervals (Fig. 7) or at  
356 firmgrounds (Fig. 9).

357 When the bioturbation degree and the sediment allow for it, the identifiable ichnoassemblage  
358 is common for the different carbonate drifts discussed herein. The carbonate drift  
359 ichnoassemblage is dominated by *Thalassinoides*, *Scolicia*, *Planolites*, *Zoophycos*, *Chondrites*,  
360 *Phycosiphon*, and *Palaeophycus*. *Taenidium* and *Nereites* may be also present according to the  
361 reports of ODP legs 166 and 194, but its recognition in cores and core photographs is not  
362 univocal (Eberli *et al.*, 1997; Isern *et al.*, 2004). Ichnogenera from different tiers typically occur  
363 together (Fig. 7). In the Maastrichtian chalk of Denmark, the occurrence of deep tiers in the  
364 assemblage is used for the differentiation of the ichnofabrics (Lauridsen *et al.*, 2011), but this  
365 is not always possible in the other study cases.

366 Among the described cases the more common infills consist of particulate organic matter and  
367 chert. Locally pyrite is present. The chert is probably the result of the dissolution of the biogenic  
368 silica of different organisms including radiolarians, diatoms, and sponge spicules (Maliva and  
369 Siever, 1989; Fabricius, 2007). Celestine is locally common in the Maldives drifts and it is

370 interpreted as the result of remobilization of fluids saturated in SrSO<sub>4</sub> during the transformation  
371 of Sr-bearing aragonite of some bioclasts into calcite (Hanor, 2004; Betzler *et al.*, 2017).

372

## 373 **5.2 Ichnofacies and Ichnofabrics**

374 The concept of ichnofacies refers to the ichnological content of the rock resulting of the activity  
375 of organisms under certain conditions of energy, nutrients, oxygenation, or sedimentation rates  
376 (MacEachern *et al.*, 2007). According to the trace assemblage reported from the different  
377 carbonate drifts (*Thalassinoides*, *Scolicia*, *Planolites*, *Zoophycos*, *Chondrites*, *Phycosiphon*,  
378 *Palaeophycus*, and minor *Taenidium* and *Nereites*), *Cruziana* and *Zoophycos* ichnofacies  
379 (Seilacher, 1967) are the dominant ichnofacies in such deposits. The *Cruziana* ichnofacies is  
380 characterized by a high diversity of trace fossils mostly a combination of deposit feeding and  
381 permanent dwelling including an assemblage as diverse as *Asterosoma*, *Chondrites*,  
382 *Cylindrichnus*, *Phoebichnus*, *Phycoides*, *Planolites*, *Rosselia*, *Rhizocoralium*, *Siphonichnus*,  
383 *Taenidium*, *Teichichnus*, *Thalassinoides*, and *Zoophycos* (Benton and Harper, 1997; Gilbert and  
384 Martinel, 1998; MacEachern *et al.*, 2007). Grazing structures as *Helminthopsis* or *Phycosiphon*  
385 are common and passive carnivore structures as *Palaeophycus* may be present (MacEachern *et*  
386 *al.*, 2007). In shallow environments with *Cruziana* ichnofacies *Arenicolites* and *Ophiomorpha*  
387 are common (MacEachern *et al.*, 2007). In contrast, the *Zoophycos* ichnofacies are dominated  
388 by feeding structures of shallow and deep tiers including *Zoophycos*, *Helminthopsis*,  
389 *Phycosiphon*, *Planolites*, *Nereites*, and minor *Chondrites*, *Scolicia*, *Thalassinoides*, and  
390 *Spyrophyton* (MacEachern *et al.*, 2007).

391 *Cruziana* ichnofacies is typical of shallow environments from tidal flats to the open offshore  
392 (Benton and Harper, 1997; MacEachern *et al.*, 2007; Gerard and Bromley, 2008). The  
393 *Zoophycos* ichnofacies is related to slope to basinal deposits, the basinward equivalent of the  
394 *Cruziana* ichnofacies (Ekdale, 1988; Goldring, 1993; MacEachern *et al.*, 2007). The trace-fossil

395 assemblages documented in carbonate drifts are a mixture of *Cruziana* and *Zoophycos*  
396 ichnofacies, but according to the dominant paleobathymetry of such deposits the *Zoophycos*  
397 ichnofacies is more representative of carbonate drifts. However, the main ecological factors,  
398 such as organic-matter input, sedimentation rate, grain size, and oxygenation vary significantly  
399 in the deep sea, especially when bottom currents are involved, and therefore such ichnofacies  
400 cannot be univocally linked to a specific water depth (Wetzel, 1983; Ekdale, 1988; Goldring,  
401 1993; MacEachern, 2007; Uchman and Wetzel, 2011).

402 As a complementary study to the ichnofacies analysis, ichnofabric analysis was applied to the  
403 studied carbonate drifts. The ichnofabrics are those aspects of the texture and internal structure  
404 of the rock resulting from all phases of bioturbation (Ekdale and Bromley, 1983), comprising  
405 the primary sedimentary conditions and the later sediment reworking during one or more phases  
406 of bioturbation (Taylor and Goldring, 1993; Taylor *et al.*, 2003; Gerard and Bromley, 2008;  
407 Buatois and Mángano, 2011; Ekdale *et al.*, 2012; Reolid and Betzler, 2018). From the  
408 ichnofabric perspective, there are three main types of ichnofabrics (IF) in carbonate drifts,  
409 including (1) completely-homogenized coarse-grained deposits, (2) intensely bioturbated fine-  
410 grained deposits; and (3) those with present to absent bioturbation and preserved sedimentary  
411 structures (Fig. 10).

412 The first type (IF1 in Table 1) includes a range of facies from coarse-grained packstone,  
413 grainstone and rudstone (Fig. 10). The bioturbation degree according to the scale of Droser and  
414 Bottjer (1986) and Hansen and MacEachern (2007) is 6 and the occurrence of discrete trace  
415 fossils is extremely rare. Discrete trace fossils are almost exclusively from the ichnogenus  
416 *Thalassinoides* and may present particulate organic matter in their infills (Fig. 5). These  
417 ichnofabrics are exclusive to the topsets of the delta drift in the Maldives.

418 The second type (IF2 in Table 1) of ichnofabrics includes facies ranging from mudstone to  
419 packstone and bioturbation degrees between 4 and 6 (Fig. 10). Ichnofabrics of packstone  
420 intervals usually present a completely-homogenized to mottled background (IF2A, bioturbation

421 index of 6). Trace fossils are hardly identifiable and usually are *Thalassinoides*- or *Planolites*-  
422 like. Fine-grained ichnofabrics, including mudstone, wackestone, and minor packstone, display  
423 a well-developed mottled background, mainly consisting on biodeformational structures  
424 overprinted by scarce trace fossils (IF2B, bioturbation indexes of 4 to 5). The main ichnogenera  
425 are *Zoophycos*, *Thalassinoides*, *Planolites*, and *Chondrites*. *Phycosiphon* and *Palaeophycus*  
426 may be present and *Taenidium* and *Nereites* are rare. The ichnofabrics do not show any clear  
427 cross-cutting relationship, and just the presence or absence of *Zoophycos* and *Chondrites* may  
428 indicate differences in the tiering. The ichnofabrics may accordingly be differentiated into  
429 shallow and deep according to the occurrence of these two ichnogenera. These ichnofabrics  
430 (IF2B) commonly intercalate with intervals completely homogenized with no or rare individual  
431 burrows (IF2A). This ichnofabric association is similar to that reported from hemipelagites  
432 (Uchman and Wetzel, 2011; Wetzel and Uchman, 2012). In the case of the very-fine grained  
433 materials of Denmark the ichnofabrics show the same alternation of heavily bioturbated  
434 sediment with poorly preserved trace fossils (Ichnofabric A of Lauridsen *et al.*, 2011) and  
435 ichnofabrics with preserved trace fossils out of the intensely bioturbated background  
436 (Ichnofabrics C of Lauridsen *et al.*, 2011). A similar bimodal distribution of completely  
437 homogenized ichnofabrics with ichnofabrics with discrete burrows is also characteristic of  
438 siliciclastic and mixed carbonate/siliciclastic drifts (Dorador and Rodríguez-Tovar, 2016).

439 The last type of ichnofabrics (IF3 in Table 1) which can be identified in carbonate drifts  
440 corresponds to the thinly laminated intervals at the bottom of the delta drift deposits at Site  
441 U1471 in the Maldives (Fig. 6), at the Lymbia section in Cyprus (Stow *et al.*, 2002), and in the  
442 Danish drifts (Damholt and Surlyk, 2004). The ichnofabric consists of fine-grained packstone  
443 with high bioturbation degree (4-6) alternating with intervals with low bioturbation index and  
444 preserved primary sedimentary structures, index from 1 to 3 (Fig. 10). The trace fossils of this  
445 ichnofabric are *Thalassinoides* and *Planolites*. The preservation of the primary structures in the  
446 carbonate drifts is rare because of the intense bioturbation. This is in a certain contrast to some

447 siliciclastic drifts, where sedimentary structures as the reported parallel fine-lamination and  
448 lenticular bedding are common (Stow and Faugères, 2008; Wetzel *et al.*, 2008).

### 449 **5.3 Paleoenvironmental interpretation**

450 The diagnostic features of the bioturbation in carbonate drifts, the ichnofacies, and the  
451 ichnofabrics are the result of a range of factors affecting the depositional environment. The two  
452 main factors affecting these deposits are the availability of organic matter and the oxygenation,  
453 both closely depending on the bottom current regime.

#### 454 *5.3.1 Ichnological content and oxygenation of carbonate drifts*

455 According to Taylor *et al.* (2003) “highly bioturbated sediment can represent no other than a  
456 well oxygenated sea floor”. The occurrence of pervasive bioturbation in carbonate drifts is  
457 therefore interpreted as the result of good sea-floor oxygenation. The high degree of  
458 bioturbation in drift deposits is likely related to the input of oxygen in the environment by  
459 bottom currents (Wetzel *et al.*, 2008; Rebesco *et al.*, 2014) which transport well-oxygenated  
460 cold-water masses (Salon *et al.*, 2008; Zenk, 2008). In contrast, drifts deposited under the  
461 influence of oxygen-poor waters, as those of polar margins are not or rarely bioturbated (Ekdale,  
462 1988; Gilbert *et al.*, 1998; Lucchi *et al.*, 2002; Lucchi and Rebesco, 2007). In summary, most  
463 environments where oxygen is not a limiting factor display moderate to high diversity of trace  
464 fossils (Ekdale, 1988), and such is the case of carbonate drifts.

#### 465 *5.3.2 Bioturbation and organic matter content*

466 In environments where the oxygen is not a limiting factor, the organic-matter content may exert  
467 a control on the intensity and type of bioturbation (Wetzel and Uchman, 1998; Taylor *et al.*,  
468 2003). In the examples discussed herein there are alternations of light and dark colored intervals  
469 (Eberli *et al.*, 1997; Isern *et al.*, 2004; Betzler *et al.*, 2017), some of them exclusively controlled  
470 by the amount of organic matter in the sediment (Betzler *et al.*, 2016, 2017). In the case of the

471 Maldives, the organic-rich dark intervals usually display high values of gamma radiation (Fig.  
472 2) and are characterized by a relatively lower degree of bioturbation with identifiable individual  
473 traces. *Zoophycos* is typical of the dark intervals and is considered as an indicator of organic  
474 matter deposition (Dorador *et al.*, 2016). *Chondrites*, also significant in these intervals, is an  
475 indicator of poor oxygenation below the sediment/water interface in the Danish drifts where  
476 they occur with small sizes (Rasmussen and Surlyk, 2012). However, as *Chondrites* always  
477 occur in intensely bioturbated sediment, it is more likely to indicate enrichment in organic  
478 matter than oxygen depletion (Uchman and Wetzel, 2011; Wetzel and Uchman, 2012). In most  
479 of the cases, the ichnofabrics with lower bioturbation indices and deeper tiers are typically result  
480 of high organic matter content (Savrda and Bottjer, 1986, 1989).

#### 481 *5.3.3 Drift sedimentation and the ichnological content*

482 The presence in the study cases of completely homogenized or mottled intervals rather than  
483 discrete burrows might be explained by lowered rates of sediment accumulation intercalated  
484 into the drift successions. Low sedimentation-rates allow bioturbation to keep pace with  
485 deposition destroying primary sedimentary structures and individual burrows (Stow and  
486 Faugères, 2008). The lithology also exerts a certain control on the type of bioturbation as  
487 sediment texture, grain size, and sorting determine the accumulation and preservation of organic  
488 matter in the sediment, and thus the ichnoassemblage and bioturbation index (Reolid and  
489 Betzler, 2018). In the Maldives drifts there is a primary lithological control on the ichnofabrics  
490 where coarser grained sediments have intensely bioturbated ichnofabrics with rare  
491 *Thalassinoides*-like burrows (IF1, Figs. 4, 5B, and 10), in contrast with the relatively more  
492 diverse ichnoassemblage documented in finer sediments (IF2B, Figs. 7 and 10). A better  
493 development of the bioturbation in fine-grained deposits seems to be a common characteristic  
494 of drift deposits independently of the composition, i.e. siliciclastic, volcanoclastic, or carbonate  
495 (Rebesco *et al.*, 2014; Rodríguez-Tovar and Hernández-Molina, 2018).

496 The consistency of sea-floor sediment also exerts a control on the bioturbation (Ekdale, 1988;  
497 Taylor *et al.*, 2003). The alternation of intervals with medium- to well-preserved traces with  
498 others completely bioturbated with rare well-preserved trace-fossils at IODP Site U1471 in the  
499 Maldives or in the carbonate drifts in Cyprus are interpreted as changes in substrate consistency  
500 associated with sedimentation breaks during drift formation (Rodríguez-Tovar and Hernández-  
501 Molina, 2018). The preservation of the trace fossils which is generally poor indicates that the  
502 surfaces of most of these carbonate drifts were soup- to softgrounds. Locally firmgrounds with  
503 well-defined traces may occur which related to omission surfaces created by enhanced currents  
504 (Eberli *et al.*, 1997; Isern *et al.*, 2004; Rodríguez-Tovar and Hernández-Molina, 2018; Reolid  
505 *et al.*, in this volume). Such omission surfaces are a distinctive feature of drift deposits  
506 elsewhere (Hüneke and Stow, 2008; Rodríguez-Tovar and Hernández-Molina, 2018).  
507 Rodríguez-Tovar and Hernández-Molina (2018) defined 6 different associations from facies  
508 with preserved primary structures (Types A-B) to completely mottled facies with softground  
509 facies (Types D-E). Firmgrounds with trace fossils with different infill than that of the  
510 surrounding sediment are the Type F for Rodríguez-Tovar and Hernández-Molina (2018). Type  
511 B according to these authors is characterized by the presence of traction sedimentary structures  
512 partly destroyed by bioturbation, and it is typical of thin beds of calcareous sandy contourites.  
513 In the Maldives there is an equivalent to this association in the laminated intervals at the base  
514 of the delta drift at Site U1471 (Fig. 6A). Primary traction sedimentary structures represent  
515 unfavorable conditions for the bioturbating organisms, in contrast with the later improvement  
516 in conditions that allows the sediment bioturbation (Fig. 6A; Rodríguez-Tovar and Hernández-  
517 Molina, 2018). Primary traction structures are also documented in the carbonate drifts of  
518 Denmark and Cyprus (Damholt and Surlyk, 2004, Hüneke and Stow, 2008). In general terms,  
519 the style of bioturbation and the type of substrate place carbonate drifts within the association  
520 types D to E of Rodríguez-Tovar and Hernández-Molina (2018). It is proposed that carbonate  
521 drifts have an additional Type G to represent the facies completely homogenized by the

522 bioturbation with rare soupground traces or mottling that occurs at the base of the drift  
523 succession in the Maldives (Fig. 4A).

#### 524 *5.3.4 Carbonate drifts and pelagites*

525 The best preservation of trace fossils documented in carbonate drifts occur in the lower part of  
526 Site U1467 in the Maldives (Fig. 7A) and in the Maastrichtian chalk of Denmark (Rasmussen  
527 and Surlyk, 2012). The location of Site U1467 in the center of the Maldives Inner Sea was  
528 probably less affected by bottom currents at the time of the deposition of the delta drift in  
529 contrast with the proximal Sites U1466 and U1468. Accordingly, the style of bioturbation of  
530 the lower sequences at this site is more similar to a pelagite or hemipelagite than to drift deposits  
531 *sensu stricto*. Pelagites are sediment deposited by pelagic settling and consist of fine-grained  
532 sediments (Rebesco *et al.*, 2014). In carbonates settings they are dominated by planktonic  
533 foraminifera, pteropods, and nannofossils (Flügel, 2004). The deep-sea sediment is commonly  
534 soft or soupy and usually well oxygenated. Accordingly, the bioturbation in such deposits  
535 consists of a mixture of discrete trace fossils mostly of the *Zoophycos/Cruziana* ichnofacies and  
536 biodeformational structures in the background (Uchman and Wetzel, 2011; Wetzel and  
537 Uchman, 2012). This kind of preservation of the bioturbation in a drift may indicate that the  
538 sedimentation is mainly dominated by pelagic settling and that currents are a secondary factor.

#### 539 *5.3.5 The role of sea-level and bottom currents on the ichnological content*

540 The recognition of the bioturbation is favored by the cyclic alternation of darker and lighter  
541 intervals as is the case at Site U1467 (Fig. 7). Such alternations may be related to changes in  
542 the intensity of the currents. Lower-energy currents allow the settling of organic matter (Fig.  
543 7F) while higher-energy currents promote the winnowing of the organic matter and the  
544 reworking and breakage of the bioclasts (Fig. 7E). The local occurrence of parallel fine-  
545 lamination and lenticular bedding in carbonate drifts is in line with the action of temporary  
546 accelerated currents (Stow *et al.*, 2002; Stow and Faugères, 2008; Wetzel *et al.*, 2008). In  
547 shallow environments such as in the delta drifts of the Maldives not only the current exerts a

548 control on the bioturbation. Changes in the base level by sea-level fluctuations or enhanced in-  
549 situ carbonate production determine the type and intensity of the bioturbation (Fig. 4C and 5B;  
550 Reolid *et al.*, this volume). In the case of the carbonate drifts of the Santaren Channel and the  
551 Marion Plateau the changes in color are related to the amount of clay in the sediment, that is  
552 determined by the energy of the currents as is the case with the organic matter in the Maldives  
553 (Eberli *et al.*, 1997; Kroon *et al.*, 2000; Isern *et al.*, 2004; John and Mutti, 2005). Similar cyclic  
554 alternation of darker and lighter colored sediment in the detached carbonate drifts of the  
555 Maldives in core NEOMA 1143 was linked to sea-level fluctuations in the Milankovitch band  
556 that control the carbonate export from the shallow water carbonate factory (Fig. 9; Betzler *et*  
557 *al.*, 2013). Thus, the changes in the sediment composition and the concomitant changes in the  
558 style of bioturbation are the result of the interplay of sea-level fluctuations that control the  
559 productivity in the shallower areas and the nature of the carbonate input and bottom currents  
560 that control the water oxygenation and the redistribution of the sediment.

561

## 562 **6. CONCLUSIONS**

563 This study of cores from carbonate drifts of the Maldives and other onshore and offshore  
564 current-controlled carbonate drifts allows for the recognition of some common bioturbation  
565 characteristics in carbonate drifts.

- 566 1. In general, the carbonate drift sediment is completely bioturbated with bioturbation  
567 indexes between 4 and 6, rarely bioturbation indexes are 1 in intervals related to  
568 enhanced bottom currents. The intensity of the bioturbation, the nature of the sediment,  
569 and the lack of contrast of carbonate grains hinders the characterization of the  
570 bioturbation.
- 571 2. The recognition of individual trace fossils against the mottled background is mostly  
572 limited to facies contacts or condensed intervals. The typical carbonate drift  
573 ichnoassemblage consists of *Thalassinoides*, *Scolicia*, *Planolites*, *Zoophycos*,

574 *Chondrites*, *Phycosiphon*, and *Palaeophycus*; *Taenidium* and *Nereites* may be also  
575 present.

576 3. The recognition of a clear tiering is difficult in carbonate drifts. Ichnogenera from  
577 different tiers typically occur together. Locally *Zoophycos* and *Chondrites* may stand as  
578 deep tiers.

579 4. The trace fossils may contain distinct infills including particulate organic-matter, pyrite,  
580 silica, and celestine.

581 5. The main ichnofacies of carbonate drifts are the *Zoophycos* ichnofacies.

582 6. There are three main types of ichnofabrics in carbonate drifts: 1) Coarse-grained and  
583 completely bioturbated sediment typical of delta drifts; 2) intensely bioturbated fine-  
584 grained deposits that may or may not present discrete trace fossils out of the mottled  
585 background; and 3) sediment with present to absent trace fossils and preserved  
586 sedimentary structures.

587 The type and intensity of the bioturbation is controlled by the amount of organic matter and the  
588 oxygenation at the seafloor. Changes in the type and intensity of the bioturbation can be used  
589 by researchers to characterize the action of bottom currents and the sea-level fluctuations  
590 affecting the carbonate factory.

591

## 592 **ACKNOWLEDGEMENTS**

593 The DFG is thanked for funding the project INDOCARB (Be1272/23-1 and -2). Many  
594 discussions with Gregor Eberli helped us to sharpen our concept. Eva Vinx is thanked for  
595 preparation of thin sections. We thank the two anonymous reviewers, the associate editor Tracy  
596 Frank, and the editor of *SEDIMENTOLOGY* Peir Pufahl for their constructive comments  
597 which helped to sharpen the concept presented in this contribution.

598

599 **REFERENCES**

- 600 **Alonso, B., Ercilla, G., Casas, D., Stow, D.A.V., Rodríguez-Tovar, F.J., Dorador, J.** and  
601 **Hernández-Molina, F.J.** (2016) Contourite vs gravity-flow deposits of the Faro Drift (Gulf of  
602 Cadiz) during the Pleistocene: sedimentological and mineralogical approaches. *Mar. Geol.* **377**,  
603 77-94.
- 604 **Anselmetti, F.S., Eberli, G.F. and Ding, Z.D.** (2000) From the Great Bahama Bank into the  
605 Straits of Florida: A margin architecture controlled by sea-level fluctuations and ocean currents.  
606 *Geol. Soc. Am. Bull.*, **112**, 829-844.
- 607 **Anderskov, K., Damholt, T. and Surlyk, F.** (2007) Late Maastrichtian chalk mounds, Stevns  
608 Klint, Denmark - Combined physical and biogenic structures. *Sed. Geol.*, **200**, 57-72.
- 609 **Aubert, O. and Droxler, A.W.** (1992) General Cenozoic evolution of the Maldives carbonate  
610 system (equatorial Indian Ocean). *Bull. Centres Rech. Explor.-Prod. Elf-Aquitaine*, **16**, 113-  
611 136.
- 612 **Benton, M. and Harper, D.A.T.** (1997) Basic Paleontology. *Geol. Magazine*, **135**, 819-842.
- 613 **Bergman, K.L., Westphal, H., Janson, X., Poiriez, A. and Eberli, G.P.** (2010) Controlling  
614 parameters on facies geometries of the Bahamas: an isolated carbonate platform environment.  
615 In: Carbonate Depositional Systems: Assessing Dimensions and Controlling Parameters (Eds  
616 H. Westphal, B. Riegl and G.P. Eberli), pp. 5–80.
- 617 **Betzler, C., Hübscher, C., Lindhorst, S., Reijmer, J.J.G., Römer, M., Droxler, A.,**  
618 **Fürstenau, J. and Lüdmann, T.** (2009) Monsoon-Induced Partial Carbonate Platform  
619 Drowning (Maldives, Indian Ocean). *Geology*, **37**, 867-870.
- 620 **Betzler, C., Lüdmann, T., Hübscher, C. and Fürstenau, J.** (2013) Current and Sea-Level  
621 Signals in Periplatform Ooze (Neogene, Maldives, Indian Ocean). *Sed. Geol.*, **290**, 126-137.

622 **Betzler, C., Lindhorst, S., Eberli, G.P., Lüdmann, T., Möbius, J., Ludwig, J., Schütter, I.,**  
623 **Wunsch, M., Reijmer, J.J.G. and Hübscher, C. (2014)** Periplatform drift: the combined result  
624 of contour current and off-bank transport along carbonate platforms. *Geology*, **42**, 871-874.

625 **Betzler, C., Eberli, G.P., Kroon, D., Wright, J.D., Swart, P.K., Nath, B.N., Alvarez-**  
626 **Zarkikian, C.A., Alonso-Garcia, M., Bialik, O.M., Blatter, C.L., Guo, J.A., Haffen, S.,**  
627 **Horoza, S., Inoue, M., Jovane, L., Lanci, L., Laya, J.C., Mee, A.L., Lüdmann, T.,**  
628 **Nakakuni, M., Niino, K., Petruny, L.M., Pratiwi, S.D., Reijmer, J.J.G., Reolid, J., Slagle,**  
629 **A.L., Sloss, C.R., Su, X., Yao, Z. and Young, J.R. (2016)** The Abrupt Onset of the Modern  
630 South Asian Monsoon Winds. *Scientific Reports*, **6**, 29838.

631 **Betzler, C., Eberli, G.P., Alvarez Zarkikian, C.A. and the Expedition 359 Scientists (2017)**  
632 Maldives Monsoon and Sea Level. Proceedings of the International Ocean Discovery Program,  
633 359: College Station, TX (International Ocean Discovery Program). [http://dx.doi.org/10.14379/](http://dx.doi.org/10.14379/iodp.proc.359.2017)  
634 [iodp.proc.359.2017](http://dx.doi.org/10.14379/iodp.proc.359.2017).

635 **Betzler, C., Eberli, G.P., Lüdmann, T., Reolid, J., Kroon, D., Reijmer, J.J.G., Swart, P.K.,**  
636 **Wright, J.D., Young, J.R., Alvarez-Zarikian, C.A., Alonso-García, M., Bialik, O.M.,**  
637 **Blättler, C.L., Guo, J.A., Haffen, S., Horozal, S., Inoue, M., Jovane, L., Lanci, L., Laya,**  
638 **J.C., Mee, A.L.H., Nakakuni, M., Nath, B.N., Niino, K., Petruny, L.M., Pratiwi, S.D.,**  
639 **Slagle, A.L., Sloss, C.R., Su, X. and Yao, Z. (2018)** Refinement of Miocene sea level and  
640 monsoon events from the sedimentary archive of the Maldives (Indian Ocean). *Progress in*  
641 *Earth and Planetary Science* **5**. DOI 10.1186/s40645-018-0165-x.

642 **Buatois, L.A. and Mángano, M.G. (2011)** Ichnology: Organism-Substrate Interactions in  
643 Space and Time. *Cambridge University Press, Cambridge*, 358 pp.

644 **Bunzel, D., Schmiedl, G., Lindhorst, S., Mackensen, A., Reolid, J., Romahn, S., Betzler,**  
645 **C. (2017)** A multi-proxi analysis of Late Quaternary ocean and climate variability for the  
646 Maldives, Inner Sea. *Clim. Past*, **13**, 1791-1813.

647 **Damholt, T. and Surlyk, F. (2004)** Laminated-bioturbated cycles in Maastrichtian chalk of the  
648 North Sea: oxygenation fluctuations within the Milankovitch frequency band. *Sedimentology*,  
649 **51**, 1323-1342.

650 **Dorador, J. and Rodríguez-Tovar, F.J. (2016)** Stratigraphic variation in ichnofabrics at the  
651 “Shackleton Site” (IODP Site U1385) on the Iberian Margin: Paleoenvironmental implications.  
652 *Mar. Geol.*, **377**, 118-126.

653 **Dorador, J., Wetzel, A. and Rodríguez-Tovar, F.J. (2016)** Zoophycos in deep-sea sediments  
654 indicates high and seasonal primary productivity: Ichnology as a proxy in palaeoceanography  
655 during glacial–interglacial variations. *Terra Nova*, **28**, 323-328.

656 **Droser, M.L. and Bottjer, D.J. (1986)** A semiquantitative field classification of ichnofabric.  
657 *J. of Sed. Petrol.*, **56**, 558-559.

658 **Duncan, R.A. and Hargraves, R.B. (1990)**  $^{40}\text{Ar}/^{39}\text{Ar}$  geochronology of basement rocks from  
659 the Mascarene Plateau, the Chagos Bank, and the Maldives Ridge. In: *Sci. Results* (Eds R.A.  
660 Duncan, J. Backman, and L.C. Peterson), *Proceedings of the Ocean Drilling Program*, **115**, 43-  
661 51.

662 **Dunham, R.J. (1962)** Classification of carbonate rocks according to depositional texture. In:  
663 *Classification of Carbonate Rocks* (Ed W.E. Ham), *AAPG Memoir*, **1**, 108-121.

664 **Eberli, G.P., Swart, P.K., McNeill, D.F., Kenter, J.A.M., Anselmetti, F.S., Melim, L.A. and**  
665 **Ginsburg, R.N. (1997)** A Synopsis of the Bahama Drilling Project: Results from two Deep

- 666 Core Borings drilled on the Great Bahama Bank. In: Proc. Ocean Drill. Program (Eds G.P.  
667 Eberli, P.K. Swart, M. Malone, *et al.*), *Init. Rep.*, **166**, 23-41.
- 668 **Eberli, G.P., Anselmetti, F.S., Isern, A.R. and Delius, H.** (2010) Timing of changes in sea-  
669 level and currents along the Miocene platforms of the Marion Plateau, Australia. In: *Cenozoic*  
670 *Carbonate Systems of Australasia* (Eds W.A. Morgan, A.D. George, P.M. Harris, J.A. Kupecz  
671 and J.E. Sarg J.E.), *SEPM Spec. Publ.*, **95**, 219-242.
- 672 **Ekdale, A.A.** (1988) Pitfalls of Paleobathimetric Interpretations Based On Trace Fossil  
673 Assemblages. *Palaios*, **3**, 464-472.
- 674 **Ekdale, A.A. and Bromley, R.G.** (1983) Trace fossils and ichnofabric in the Kjølby Gaard  
675 Marl, uppermost Cretaceous, Denmark. *Bull. geol. Soc. Denmark*, **31**, 107-119.
- 676 **Ekdale, A.A., Bromley, R. and Knaust, D.** (2012) The ichnofabric concept. In: *Trace Fossils*  
677 *as Indicators of Sedimentary Environments* (Eds D. Knaust and R.G. Bromley), *Dev.*  
678 *Sedimentol.*, **64**, 139-155.
- 679 **Embry, A.F. and Klovan, J.E.** (1972) Absolute water depth limits of late Devonian ecological  
680 zones. *Geologische Rundschau*, **61**, 672-686.
- 681 **Fabricius, I. L.** (2007). Chalk: composition, diagenesis and physical properties. *Bull. Geol.*  
682 *Soc. Denmark*, **55**, 97-128.
- 683 **Flügel, E.** (2004) Microfacies of carbonate rocks: analysis, interpretation and application.  
684 *Springer, New York*, 976 pp.
- 685 **Gerard, J. and Bromley, R.** (2008) Ichnofabrics in Clastic Sediments: Application to  
686 Sedimentological Core Studied (Ed J. Gerard), *Madrid*, 100 pp.

- 687 **Gilbert, J.M. and Martinel, J.** (1998) The ichnofacies model, 30 years later. *Revista Española*  
688 *de Paleontología*, **13**, 167-174.
- 689 **Gilbert, I.M., Pudsey, C.J. and Murray, J.** (1998) A sediment record of cyclic bottom-current  
690 variability from the northwest Weddell Sea. *Sed. Geol.*, **115**, 185-214.
- 691 **Goldring, R.** (1993) Ichnofacies and Facies Interpretation. *Palaios*, **8**, 403-405.
- 692 **Hanor, J.S.** (2004) A model for the origin of large carbonate- and evaporite-hosted celestine  
693 (SrSO<sub>4</sub>) deposits. *J. Sed. Res.*, **74**, 168-175.
- 694 **Hansen, C.D. and MacEachern, J.A.** (2007) Application of the asymmetric delta model to  
695 along-strike facies variations in a mixed wave- and river-influenced delta lobe, Upper  
696 Cretaceous Basal Belly River Formation, central Alberta. In: *Applied Ichnology* (Eds J.A.  
697 MacEachern, K.L. Bann and S.G. Pemberton), *SEPM Short Course Notes*, **52**, 256-272.
- 698 **Huneke, N.V. and Stow, D.A.V.** (2008) Identification of ancient contourites: problems and  
699 palaeoceanographic significance. In: *Contourites* (Eds M. Rebesco and A. Camerlenghi), *Dev.*  
700 *Sedimentol.*, **60**, 323-344.
- 701 **Isern, A., Anselmetti, F.S. and Blum, P.** (2004) A Neogene carbonate platform, slope and shelf  
702 edifice shaped by sea level and ocean currents, Marion Plateau (Northeast Australia). In:  
703 *Seismic imaging of carbonate reservoirs and systems* (Eds G.P. Eberli, J.L. Masafferro and J.F.  
704 Sarg), *AAPG Mem.*, **81**, 291-307.
- 705 **John, C.M. and Mutti, M.** (2005) The response of heterozoan carbonate systems to  
706 Paleooceanographic, climatic and eustatic changes: a perspective from slope sediments of the  
707 Marion Plateau (ODP Leg 194). *J. Sed. Res.*, **75**, 51-65.
- 708 **Kahler, G. and Stow, D.A.V.** (1998) Turbidites and contourites of the Paleogene Lefkara  
709 Formation, southern Cyprus. *Sed. Geol.*, **115**, 215-231.

710 **Knaust, D.** (2012) Methodology and techniques. In: *Trace Fossils as Indicators of Sedimentary*  
711 *Environments* (Eds D. Knaust and R.G. Bromley), *Dev. Sedimentol.*, **64**, 245-271.

712 **Kroon, D., Willians, T., Pirmez, C., Spezzaferri, S., Sato, T. and Wright, J.D.** (2000)  
713 Coupled early Pliocene-middle Miocene bio-cyclostratigraphy of site 1006 reveals orbitally  
714 induced cyclicity patterns of Great Bahama Bank carbonate production. In: *Sci. Results* (Eds  
715 P.K. Swart, G.P. Eberli, M.J. Malone and J.F. Sarg), *Proc. ODP*, **166**, 155-165.

716 **Lauridsen, B.W., Surlyk, F. and Bromley, R.G.** (2011) Trace fossils of a cyclic chalk-marl  
717 succession; the upper Maastrichtian Rørdal Member, Denmark. *Cretaceous Res.*, **32**, 194-202.

718 **Lucchi, R.G. and Rebesco, M.** (2007) Glacial contourites on the Antarctic Peninsula margin:  
719 insight for palaeoenvironmental and palaeoclimatic conditions. In: *Economic and*  
720 *Palaeoceanographic Significance of Contourite Deposits* (Eds A.R. Viana and M. Rebesco),  
721 *Geol. Soc. London Special Publ.*, **276**, 111-127.

722 **Lucchi, R.G., Rebesco, M., Camerlenghi, A., Busetti, M., Tomadin, L., Villa, G., Persico,**  
723 **D, Morigi, C., Bonci, M.C. and Giorgetti, G.** (2002). Mid-late Pleistocene glacimarine  
724 sedimentary processes of a high-latitude, deep-sea sediment drift (Antarctic Peninsula Pacific  
725 margin). *Mar. Geol.*, **189**, 343-370.

726 **Lüdmann, T., Wiggershaus, S., Betzler, C. and Hübscher, C.** (2012) Southwest Mallorca  
727 Island: a cool-water carbonate margin dominated by drift deposition associated with giant mass  
728 wasting. *Mar. Geol.*, **307-310**, 73-87.

729 **Lüdmann, T., Kalvelage, C., Betzler, C., Fürstenau, J. and Hübscher, C.** (2013) The  
730 Maldives, a Giant Isolated Carbonate Platform Dominated by Bottom Currents. *Mar. Petrol.*  
731 *Geol.*, **43**, 326-340.

732 **Lüdmann, T., Betzler, C., Eberli, G.P., Reolid, J., Reijmer, J.J.G., Sloss, C.R., Bialik,**  
733 **O.M., Alvarez-Zarkikian, C.A., Alonso-Garcia, M., Blatter, C.L., Guo, J.A., Haffen, S.,**  
734 **Horozal, S., Inoue, M., Jovane, L., Kroon, D., Lanci, L., Laya, J.C., Mee, A.L., Nakakuni,**  
735 **M., Nath, B.N., Niino, K., Petruny, L.M., Pratiwi, S.D., Slagle, A.L., Su, X., Swart, P.K.,**  
736 **Wright, J.D., Yao, Z. and Young, J.R. (2018) Carbonate delta drifts: a new drift type. *Mar.*  
737 *Geol.*, **401**, 98-111.**

738 **MacEachern, J.A., Pemberton, S.G., Gingras, M.K., Bann, K.L. and Dafoe, L.T. (2007)**  
739 **Use of trace fossils in genetic stratigraphy. In: *Trace Fossils. Concepts, Problems, Prospects***  
740 **(Ed. W. Miller.), Elsevier, *Amsterdam*, pp. 105-128.**

741 **Maliva, R.G. and Siever, R. (1989) Nodular chert formation in carbonate rocks. *J. of Geol.*,**  
742 **97, 421-433.**

743 **Mulder, T., Ducassou, E., Hanquiez, V., Principaud, M., Fauquembergue, K.,**  
744 **Tournadour, E., Chabaud, L., Reijmer, J.J.G., Recouvreur, A., Gillet, H., Borgomano, J.**  
745 **and Schmitt, A. (submitted) Contour current imprints and contourite drifts in the Bahamian**  
746 **Archipelago.**

747 **Mullins, H.T., Neumann, A.C., Wilber, R.J., Hine, A.C. and Chinburg, A.J. (1980)**  
748 **Carbonate sediment drifts in northern Straits of Florida. *Bull. Am. Assoc. Pet. Geol.*, **64**, 1701-**  
749 **1717.**

750 **Paulat, M., Lüdmann, T., Betzler, C. and Eberli, G.P. (submitted) Neogene**  
751 **paleoceanographical changes recorded in a carbonatic contourite drift (Santaren Channel,**  
752 **Bahamas).**

753 **Pemberton, S.G., MacEachern, J.A., Gingras, M.K. and Saunders, T.D.A. (2008) Biogenic**  
754 **chaos: Cryptobioturbation and the work of sedimentologically friendly organisms.**  
755 ***Palaeogeogr., Palaeoclimatol., Palaeoecol.*, **270**, 273-279.**

756 **Purdy, E.G. and Bertram, G.T.** (1993) Carbonate Concepts from the Maldives, Indian Ocean.  
757 *AAPG Studies in Geology*, **34**, 56 pp.

758 **Rasmussen, S.L. and Surlyk, F.** (2012) Facies and ichnology of an Upper Cretaceous chalk  
759 contourite drift complex, eastern Denmark, and the validity of contourite facies models. *J. Geol.*  
760 *Soc. Lond.*, **169**, 435-447.

761 **Rebesco, M.** (2005) Contourites. In: Encyclopedia of Geology 4 (Eds. R.C. Selby, L.R.M.  
762 Cocks, L.R. Plimer), Elsevier, *Oxford*, pp. 513-527.

763 **Rebesco, M., Camerlenghi, A.** (Eds.), 2008. Contourites. *Dev.Sedimentol.*, **60**, 663 pp.

764 **Rebesco, M., Hernández-Molina, F.J., Van Rooij, D. and Wåhlin, A.** (2014) Contourites and  
765 associated sediments controlled by deep-water circulation processes: State-of-the-art and future  
766 considerations. *Mar. Geol.*, **352**, 111-154.

767 **Reolid, J. and Betzler, C.** (2018) Ichnofabrics logs for the characterization of the organic  
768 content in carbonates. *Mar. Petrol. Geol.*, **95**, 246-254.

769 **Reolid, J., Reolid, M., Betzler, C., Lindhorst, S., Wiesner, M. G. and Lahajnar, N.** (2017)  
770 Upper Pleistocene cold-water corals from the Inner Sea of the Maldives: taphonomy and  
771 environment, *Facies*, **63**, 1-20.

772 **Reolid, J., Betzler, C., Lüdmann, T. and Bohlen, M.** (submitted) Sedimentology of carbonate  
773 delta drifts.

774 **Rodríguez-Tovar, F.J. and Hernández-Molina, F.J.** (2018) Ichnological analysis of  
775 contourites: Past, present and future. *Earth-Sci. Rev.*, **182**, 28-41.

776 **Salon, S., Crise, A. and Van Loon, A.J.** (2008) Dynamics of the bottom boundary layer. In:  
777 *Contourites* (Eds M. Rebesco and A. Camerlenghi), *Dev. Sedimentol.*, **60**, 83-97.

- 778 **Savrda, C.E. and Bottjer, D.J.** (1986) Trace fossil model for reconstruction of  
779 palaeooxygenation in bottom-waters. *Geology*, **14**, 3-6.
- 780 **Savrda, C.E. and Bottjer, D.J.** (1989) Anatomy and implications of bioturbated beds in 'black  
781 shale' sequences: examples from the Jurassic Posidonienschiefer (southern Germany). *Palaios*,  
782 **4**, 330-342.
- 783 **Seilacher, A.** (1967) Bathymetry of trace fossils. *Mar. Geol.*, **5**, 413-428.
- 784 **Stow, D.A.V. and Faugères, J. C.** (2008) Contourite facies and the facies model, In:  
785 *Contourites* (Eds M. Rebesco and A. Camerlenghi), *Dev. Sedimentol.*, **60**, 223-256.
- 786 **Stow, D.A.V., Faugères, J.-C., Viana, A.R. and Gonthier, E.** (1998) Fossil contourites: a  
787 critical review. *Sediment. Geol.*, **115**, 3-31.
- 788 **Stow, D.A.V., Kahler, G. and Reeder, M.** (2002). Fossil contourites: type example from an  
789 Oligocene palaeoslope system, Cyprus. In: *Deep-Water Contourite Systems: Modern Drifts and*  
790 *Ancient Series, Seismic and Sedimentary Characteristics* (Eds D.A.V. Stow, C.J. Pudsey, J.A.  
791 Howe, J.C. Faugères and A.R. Viana), *Geol. Soc. London Memoirs*, **22**, 443-455.
- 792 **Surlyk, F. and Lykke-Andersen, H.** (2007) Contourite drifts, moats and channels in the Upper  
793 Cretaceous chalk of the Danish Basin. *Sedimentology*, **54**, 405-422.
- 794 **Taylor, A.M. and Goldring, R.** (1993) Description and analysis of bioturbation and  
795 ichnofabric. *J. Geol. Soc.*, **150**, 141-148.
- 796 **Taylor, A.M., Goldring, R. and Gowland, S.** (2003) Analysis and application of ichnofabrics.  
797 *Earth-Sci. Rev.*, **60**, 227-259.

798 **Uchman, A. and Wetzel, A.** (2011) Deep-sea ichnology: the relationships between depositional  
799 environment and endobenthic organisms. In: *Deep-Sea Sediments* (Eds H. Hüneke and T.  
800 Mulder). *Dev. Sedimentol.*, **63**, 517-556.

801 **Viana, A.R. and Rebesco, M.** (2007) Economic and palaeoceanographic significance of  
802 contourite deposits. *Geol. Soc., London, Special Publication*, **276**, 350 pp.

803 **Wetzel, A.** (1983) Biogenic sedimentary structures in a modern upwelling region: NW African  
804 continental margin. In: *Coastal Upwelling and Its Sediment Record* (Eds J. Thiede and E.  
805 Suess), *Part B: Sedimentary Records of Ancient Coastal Upwelling. Plenum, New York*, 123-  
806 144.

807 **Wetzel, A. and Uchman, A.** (2012) Hemipelagic and pelagic basin plains. In: *Trace Fossils as*  
808 *Indicators of Sedimentary Environments* (Eds D. Knaust and R.G. Bromley), *Dev. Sedimentol.*,  
809 **64**, 673-701.

810 **Wetzel, A., Werner, F. and Stow, D.A.V.** (2008) Bioturbation and biogenic sedimentary  
811 structures in contourites. In: *Contourites* (Eds M. Rebesco and A. Camerlenghi), *Dev.*  
812 *Sedimentol.*, **60**, 183-202.

813 **Zenk, W.** (2008) Abyssal and contour currents. In: *Contourites* (Eds M. Rebesco and A.  
814 Camerlenghi), *Dev. Sedimentol.*, **60**, 35-57.

815

816

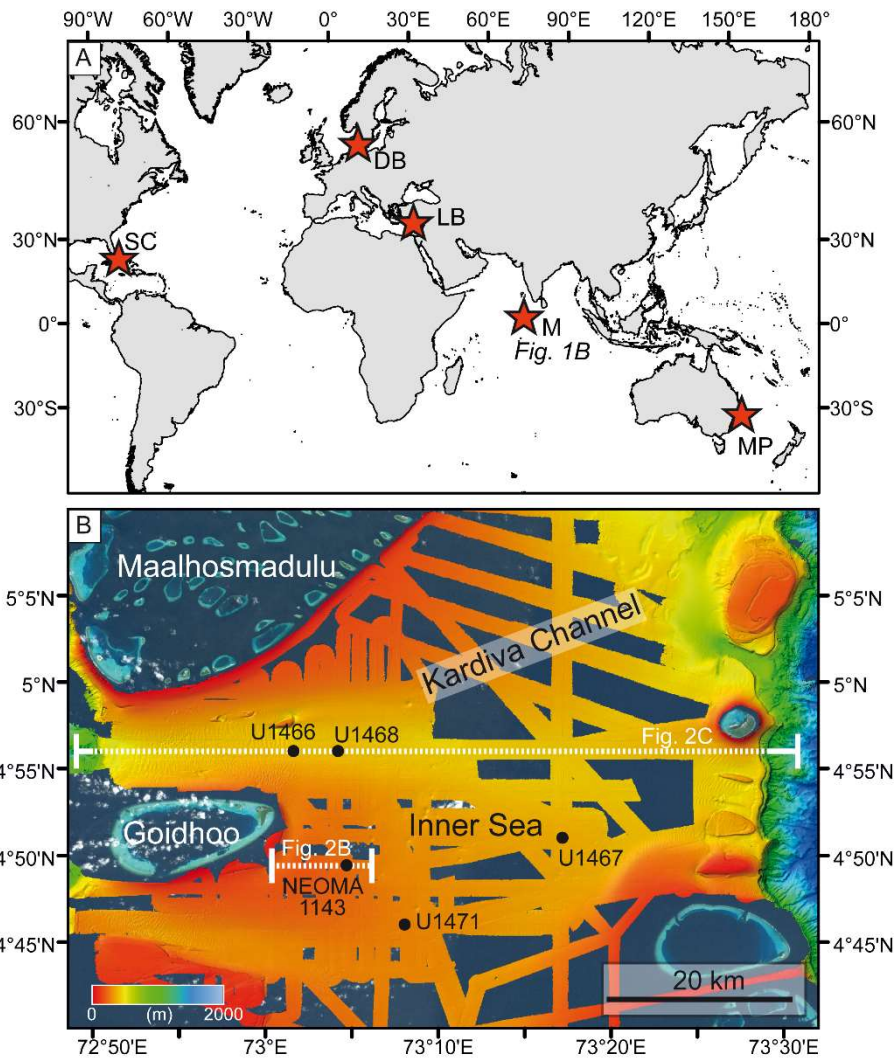
817

818

819

820

821 **FIGURES**



822

823 **Figure 1:** A Location of the carbonate drifts studied in this work. From left to right: the drifts  
824 at Santaren Channel (SC) lining Great Bahama Bank, the drifts of the Danish basin (DB) in  
825 Denmark, the drifts of the Limassol and Larnaca Basins (LB) in Cyprus, the drifts of the Inner  
826 Sea of the Maldives (M), and those of the Marion Plateau (MP) in Australia. B Close up of the  
827 study area of the Maldives with the location of the study sites and seismic lines in Figure 2.

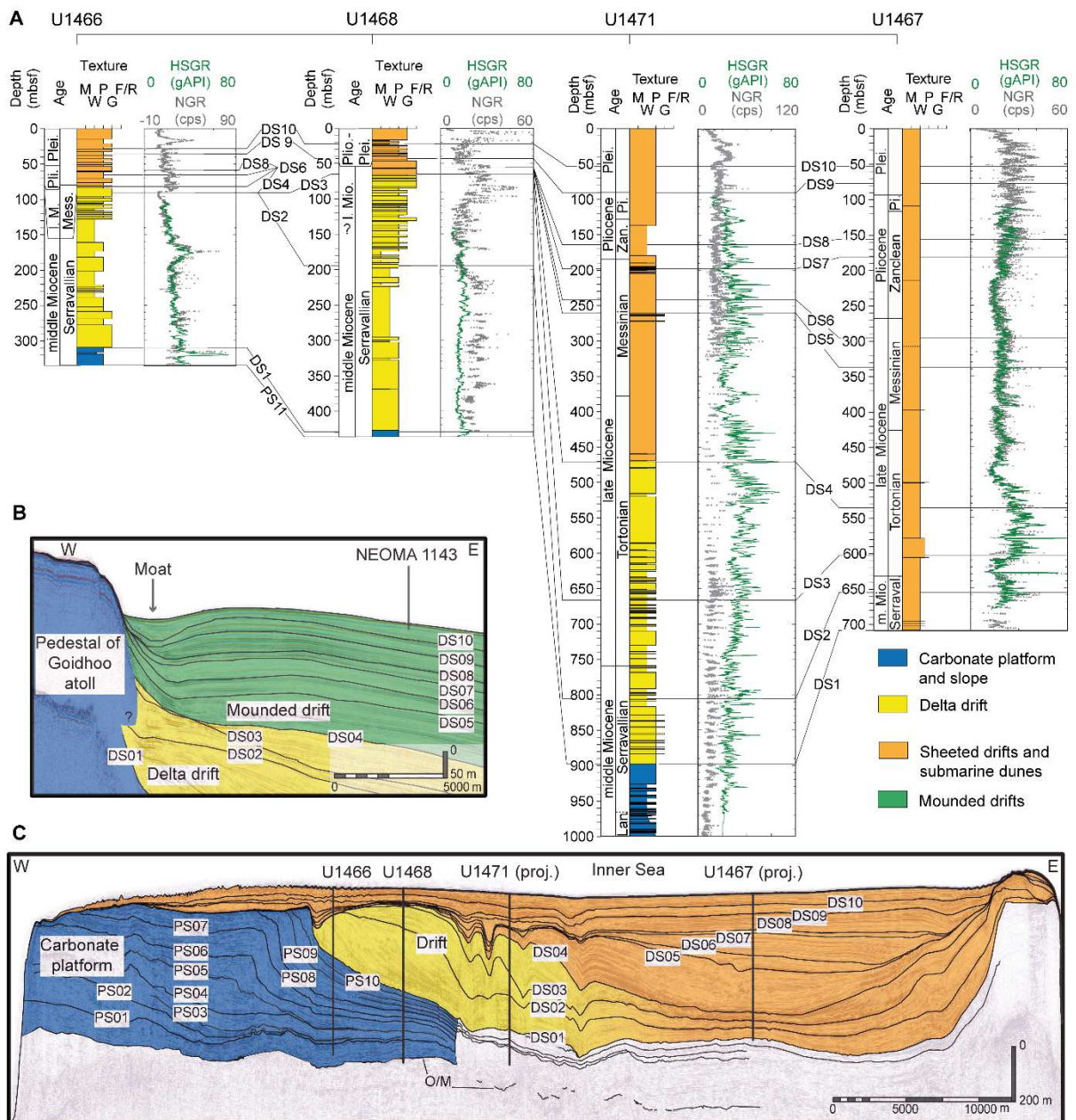
828

829

830

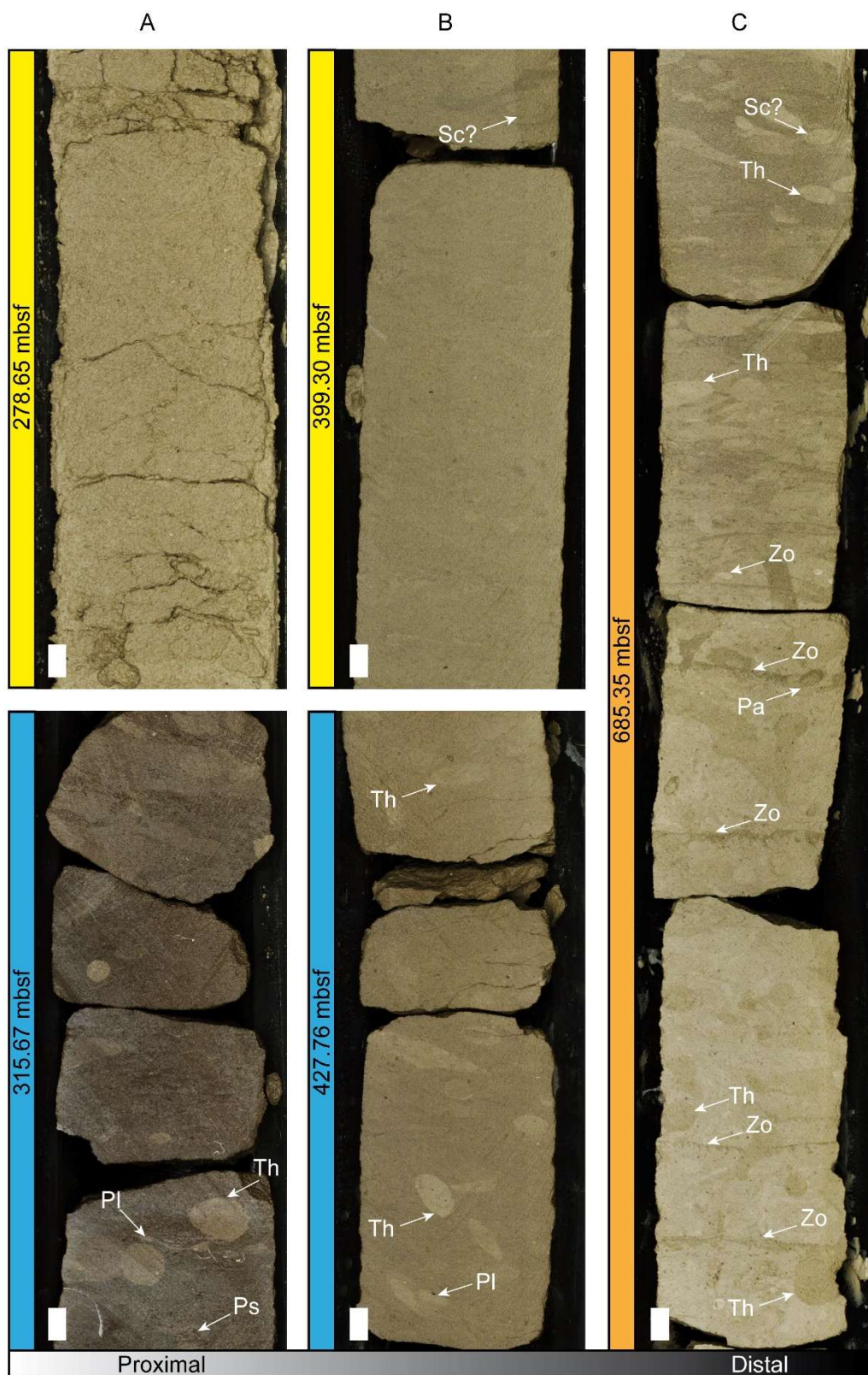
831

832



833

834 **Figure 2:** A Lithological columns of the IODP sites cored in the drift deposits of the Maldives  
 835 (modified after Betzler *et al.*, 2018). Each profile includes depth (mbsf), age, sediment texture,  
 836 and natural gamma radiation from downhole logs (HSGR) and core gamma measurements (NGR). The  
 837 sequence boundaries of the platform (PS) and drift sequences (DS) are marked by horizontal  
 838 lines. For definition of these boundaries see Betzler *et al.* (2017). **B** Seismic line P54 (location  
 839 in Fig. 1) showing the position of NEOMA core 1143 in a mounded drift (modified after Betzler  
 840 *et al.*, 2013). **C** Seismic line P65 (Location in Fig. 1) showing the positions of the studied IODP  
 841 Sites drilled in delta and sheeted drift deposits (modified after Betzler *et al.*, 2018).



843

844 **Figure 3:** Core photographs of the facies and bioturbation changes of the bottom part of the  
 845 delta drift (yellow) of the Maldives from the proximal Site U1466 (A) to U1468 (B), and the

846 sheeted drifts (orange) at the distal Site U1467 (C). Figures 3A and 3B also display the directly  
847 underlying slope sediments (blue) to evidence the increase in the bioturbation degree from the  
848 slope to the drift deposits. The main ichnotaxa are *Phycosiphon* (Ps), *Palaeophycus* (Pa),  
849 *Planolites* (Pl), *Thalassinoides* (Th), *Scolicia* (Sc), and *Zoophycos* (Zo). Scale bar =1 cm.

850

851

852

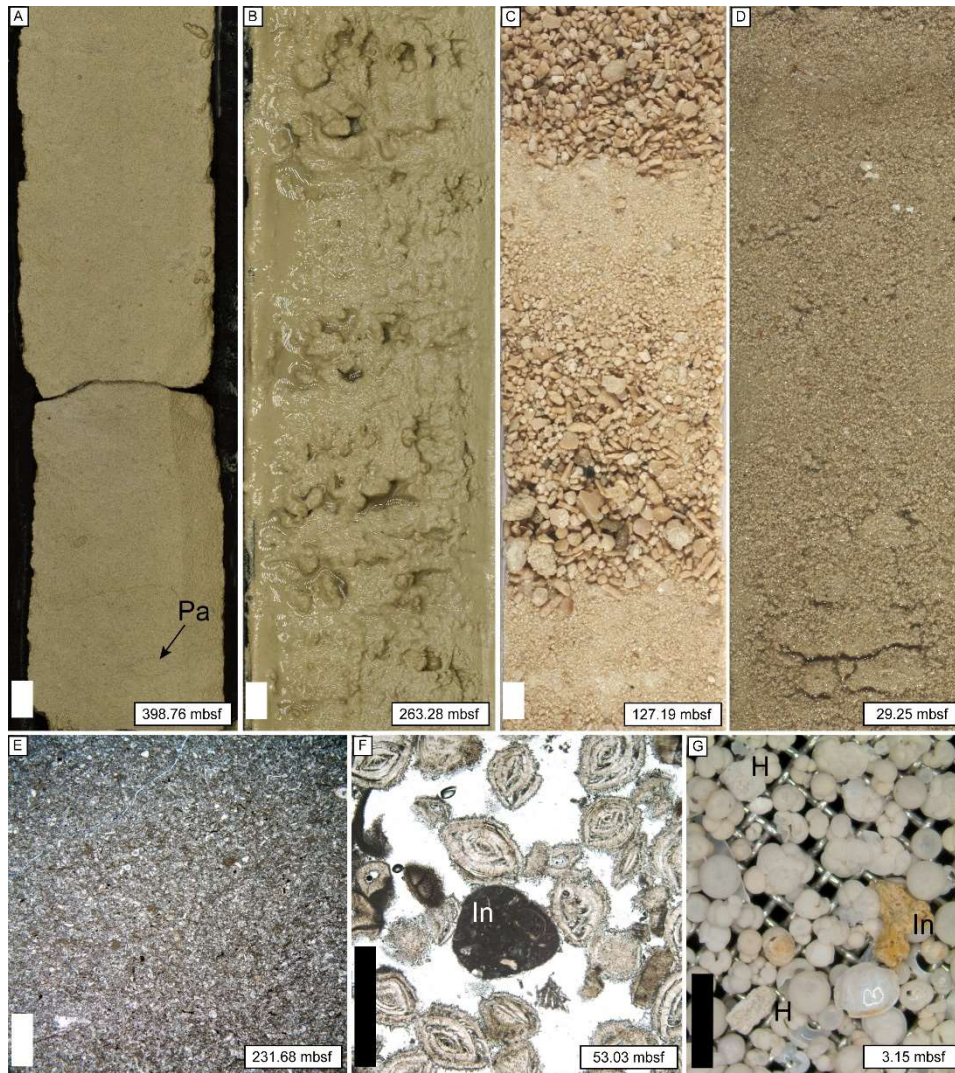
853

854

855

856

857



858

859 **Figure 4:** Facies of the delta and sheeted drift at the proximal IODP sites (U1466 and U1468)  
 860 of the Maldives modified after Lüdmann *et al.* (2018) (scale bar for core photographs=1 cm,  
 861 scale bar for photomicrographs=1 mm). **A** Core photograph of a fine-grained bioclastic  
 862 packstone at Site U1468. **B** Core photograph of an unlithified wackestone with intraclasts at  
 863 Site U1468. **C** Core photograph of a large benthic foraminifera-rich rudstone to grainstone with  
 864 a fining upward grain size trend at Site U1468. Echinoid spines, large benthic foraminifera and  
 865 intraclasts are common. **D** Core photograph of a partially lithified packstone to grainstone at  
 866 Site U1468. The better lithified areas probably correspond to *Thalassinoides* burrows. **E**  
 867 Photomicrograph of the fine-grained packstone at Site U1466. **F** Photomicrograph of the  
 868 rudstone to grainstone facies at U1468 with abundant *Amphistegina* and intraclasts (In). **G**

869 Photomicrograph of a grainstone to packstone at Site U1468 with abundant planktonic  
870 foraminifera and *Halimeda* plates (H) and intraclasts.

871



872

873 **Figure 5:** Distinct infills in traces from the carbonate drifts of the Maldives (scale bar=1 cm).

874 **A** *Thalassinoides* preserved in chert at Site U1468. **B-C** ?*Thalassinoides* burrows enriched in  
875 particulate organic matter at Site U1468 (B) and U1471 (C). **D** *Thalassinoides* preserved in  
876 celestine at Site U1471.

877

878

879

880

881

882

883

884

885

886



887

888 **Figure 6:** Facies and bioturbation of the drift deposits at Site U1471 of the Maldives (scale  
889 bar=1 cm). **A** Core photograph of alternating intensely bioturbated grainstone/packstone  
890 intervals with finely laminated packstone intervals. Trace fossils in the laminated intervals are  
891 infilled by the overlying grainstone. **B** Core photograph of an almost completely homogenized  
892 packstone with rare discrete trace fossils. **C** Core photograph of bioturbated packstone without  
893 discrete trace fossils. **D** Core photograph of a mottled packstone. *Phycosiphon* (Ps), *Planolites*  
894 (Pl), *Thalassinoides* (Th), and *Zoophycos* (Zo).

895

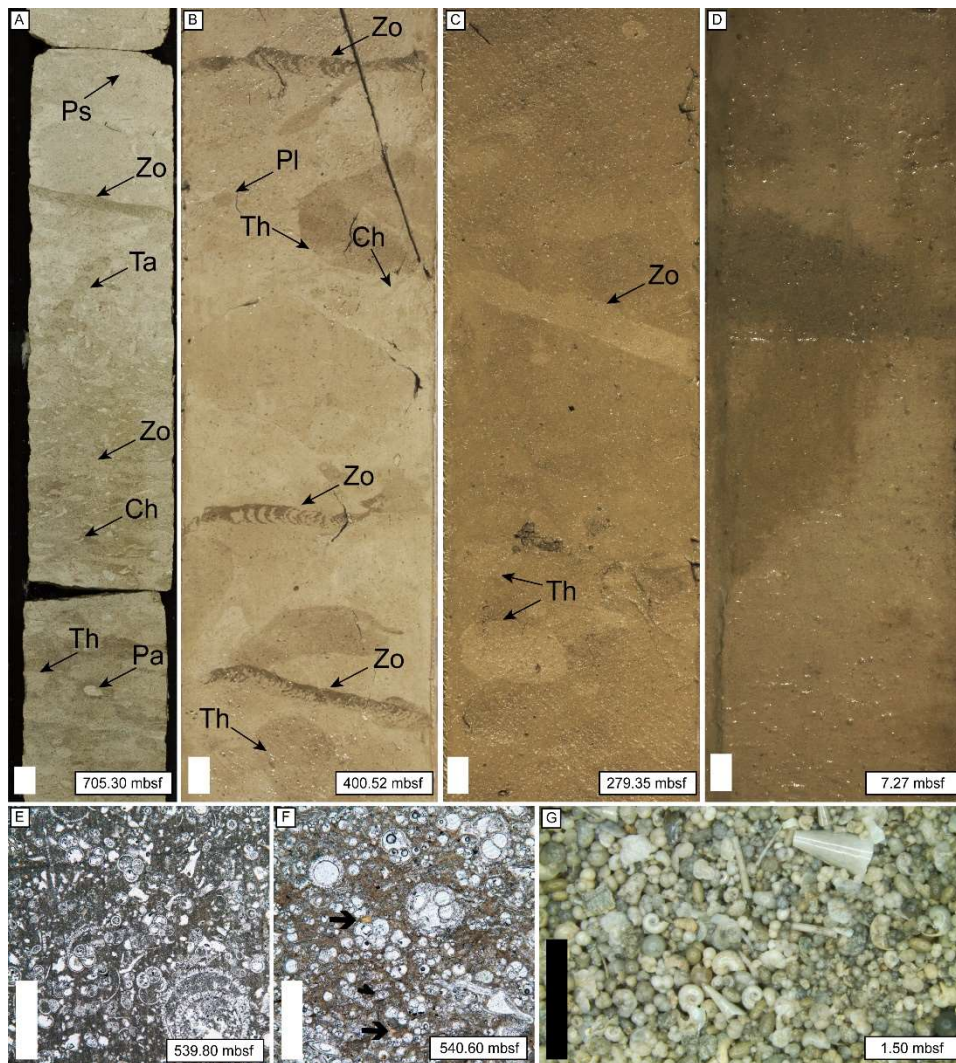
896

897

898

899

900



901

902 **Figure 7:** Facies and bioturbation of the sheeted drift deposits at Site U1467 in the Maldives

903 (scale bar for core photographs=1 cm, scale bar for photomicrographs=1 mm, black bar=1 cm).

904 **A** Core photograph of a dark- and a light-colored interval of fine-grained wackestone with

905 abundant discrete trace fossils. **B** Core photograph of fine-grained wackestone with abundant

906 *Zoophycos* out of the heavily bioturbated background. **C** Core photograph intensely bioturbated

907 wackestone with diffuse trace fossils out of the mottled background. **D** Core photograph of an

908 unlithified wackestone with large trace fossils (*Thalassinoides?*). **E** Photomicrograph of a light

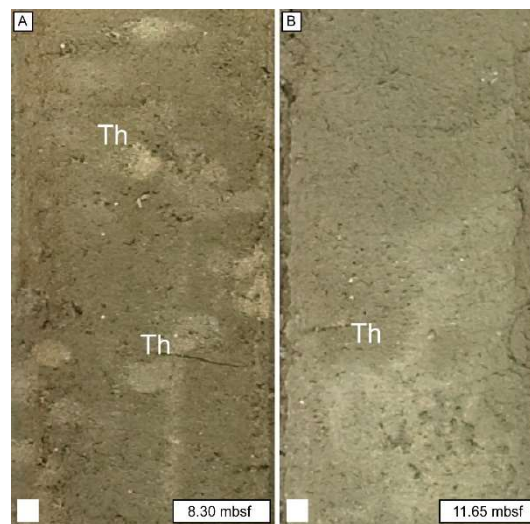
909 interval of a fine-grained wackestone. Note the extensive fragmentation of the planktonic

910 foraminifera. **F** Photomicrograph of a dark interval of the fine-grained wackestone with

911 preserved organic matter and fish debris (black arrow). **G** Photomicrograph of a grainstone

912 from the uppermost part of the drift with abundant pelagic fauna including planktonic

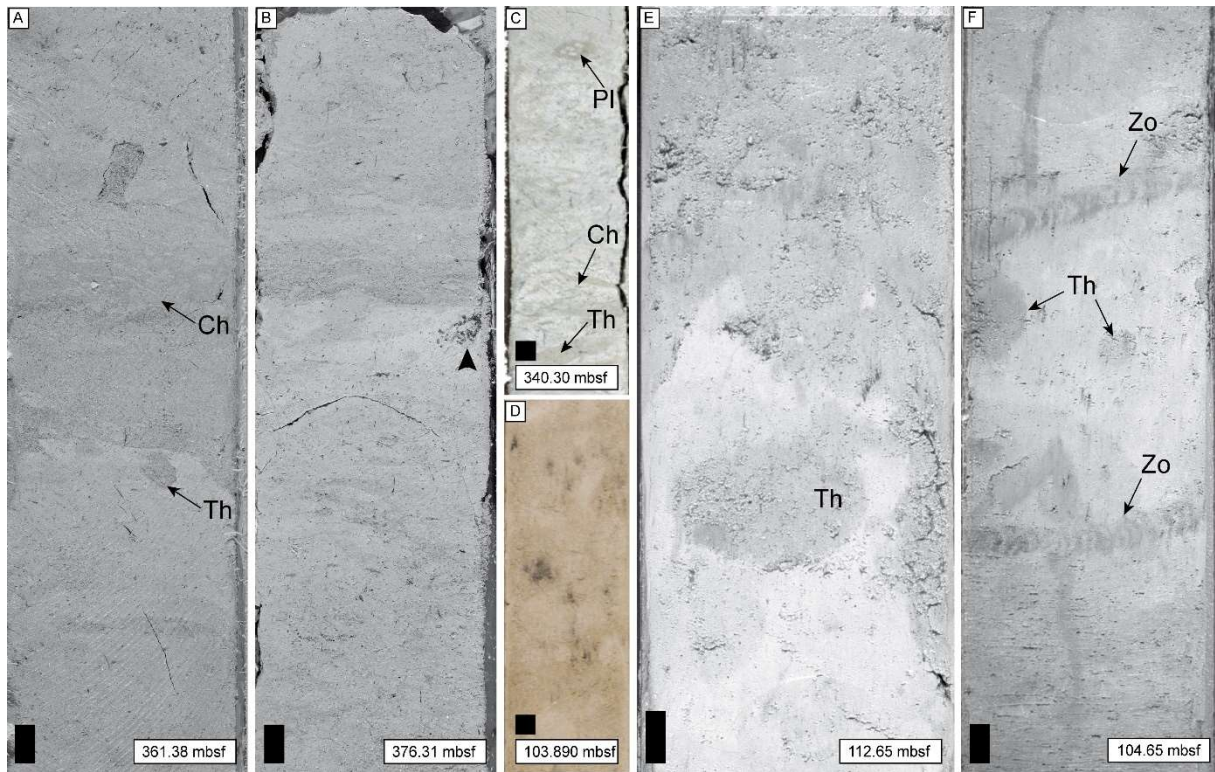
913 foraminifera and pteropods. The main ichnotaxa are *Chondrites* (Ch), *Palaeophycus* (Pa),  
914 *Phycosiphon* (Ps), *Planolites* (Pl), *Taenidium* (Ta), *Thalassinoides* (Th), and *Zoophycos* (Zo).



915

916 **Figure 8:** Facies and bioturbation of the detached drift recovered by core NEOMA 1143 in the  
917 Maldives (scale bar=1 cm). **A** Fine-grained ooze with some large bioclast and traces of  
918 *Thalassinoides* out of the mottled background. **B** Contact between light (aragonite-rich) and  
919 dark (aragonite-poor) sediment. The traces of *Thalassinoides* in the light interval are infilled by  
920 the overlying dark material.

921



922

923 **Figure 9:** Representative facies and bioturbation of drift from Bahamas and Australia (scale  
 924 bar=1 cm). **A-B** Core photograph of a firmground at Site 1006A in the Santaren drift of  
 925 Bahamas. The firmground was burrowed and the overlying sediment is mostly bioturbated by  
 926 *Chondrites* (A). The black arrow-head indicates trace fossils preserved in pyrite (B). **C** Core  
 927 photograph of heavily bioturbated wackestone/packstone with diverse trace fossils at Site 1006  
 928 in Bahamas. **D** Core photograph of a mottled wackestone at Site 1195B in Australia with  
 929 accumulation of particulate organic matter in trace fossils (*Thalassinoides*?). **E** Core photograph  
 930 of a firmground at Site 1192A. **F** Core photograph of a bioturbated wackestone with discrete  
 931 trace fossils out of the mottled background. *Chondrites* (Ch), *Planolites* (Pl), *Thalassinoides*  
 932 (Th), and *Zoophycos* (Zo).

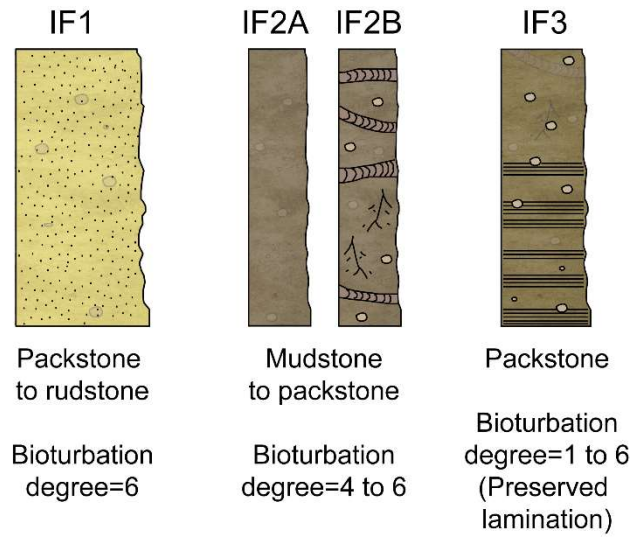
933

934

935

936

937



938

939 **Figure 10:** Schematic model of the main ichnofabrics observed in carbonate drifts. Bioturbation  
 940 index according to Droser and Bottjer (1986). The different trace fossils illustrate the  
 941 occurrence of distinctive bioturbation out of the mottled background.

942

943

944

945

946

947

948

949

950

951

952

953

954

955

956 **Table 1.** Summary of main types of carbonate drifts and their ichnological and sedimentological  
 957 features (facies, bioturbation index, main ichnogenera, and ichnofabrics).  
 958

<b>Drift type</b>	<b>Sediment texture</b>	<b>Bioturbation index (BI)</b>	<b>Main ichnogenera</b>	<b>Ichnofabrics (IF)</b>
Delta drift.	Fine-grained packstone to coarse-grained grainstone to rudstone.	5-6 Locally 1-3 in laminated intervals.	<i>Thalassinoides</i> , <i>Planolites</i> , <i>Zoophycos</i> , <i>Chondrites</i> , <i>Phycosiphon</i> , and <i>Palaeophycus</i> in fine-grained facies. <i>Thalassinoides</i> in coarse-grained facies.	<b>IF1</b> Coarse-grained sediment is completely bioturbated (BI=6) rarely with <i>Thalassinoides</i> traces. <b>IF2</b> Alternation of ichnofabrics 2A and 2B <b>IF2A</b> Fine-grained material completely bioturbated (BI=6) with local <i>Thalassinoides</i> - and <i>Planolites</i> -like traces. <b>IF2B</b> Fine-grained sediment intensely bioturbated (BI=4-5)

			with diverse trace fossils.
			<b>IF3</b> Fine-grained sediment with low bioturbation (BI=1-3) and preserved primary sedimentary structures.
Sheeted drift.	Fine-grained wackestone to packstone. 4-6.	<i>Thalassinoides</i> , <i>Scolicia</i> , <i>Planolites</i> , <i>Zoophycos</i> , <i>Chondrites</i> , <i>Phycosiphon</i> , and <i>Palaeophycus</i> . <i>Taenidium</i> and <i>Nereites</i> may be also present. <i>Ophiomorpha</i> and <i>?Helminthoides</i> may be present in drifts reworking calciturbidites.	<b>IF2</b> Alternation of ichnofabrics 2A and 2B <b>IF2A</b> Fine-grained material completely bioturbated (BI=6) with local <i>Thalassinoides</i> - and <i>Planolites</i> -like traces. <b>IF2B</b> Fine-grained sediment intensely bioturbated (BI=4-5) with diverse trace fossils.
Mounded drift.	Chalk-ooze. 4-6 Fine-grained	<i>Thalassinoides</i> , <i>Scolicia</i> , <i>Planolites</i> , <i>Zoophycos</i> ,	<b>IF2</b> Alternation of ichnofabrics 2A and 2B

---

wackestone	Locally 2-3 in	<i>Chondrites</i> ,	<b>IF2A</b> Fine-grained
to packstone.	laminated	<i>Phycosiphon</i> , and	material completely
	intervals.	<i>Palaeophycus</i> .	bioturbated (BI=6)
		<i>Asterosoma</i> may be	with local
		present.	<i>Thalassinoides</i> - and
			<i>Planolites</i> -like traces.
			<b>IF2B</b> Fine-grained
			sediment intensely
			bioturbated (BI=4-5)
			with diverse trace
			fossils.
			<b>IF3</b> Fine-grained
			sediment with low
			bioturbation (BI=2-3)
			and preserved
			primary sedimentary
			structures.

---

959

960

961

962

963

964

965

966

967

968 **Table 2.** List of the main ichnological features in carbonate

- 
1. Completely bioturbated sediment with bioturbation indexes between 4 and 6.

---

  2. Distinctive trace fossils against the mottled background are limited to facies contacts or condensed intervals. The intense bioturbation, lack of contrast of the carbonate sediment, and diagenesis difficult the identification of trace fossils.

---

  3. The typical ichnoassemblage consists of *Thalassinoides*, *Scolicia*, *Planolites*, *Zoophycos*, *Chondrites*, *Phycosiphon*, and *Palaeophycus*. *Taenidium* and *Nereites* may be also present.

---

  4. Ichnogenera from different tiers typically occur together, only *Zoophycos* and *Chondrites* may locally stand as deep tiers.

---

  5. Trace fossils may present distinct infills including particulate organic-matter, pyrite, silica, and celestine.

---

  6. *Cruziana* and *Zoophycos* are the main ichnofacies.

---

  7. The ichnofabrics grade from coarse-grained and completely bioturbated to ichnofabrics with present to absent trace fossils and preserved sedimentary structures.

969